ACCESSIBILITY:
Open

OsloMet – Oslo Metropolitan University

Department of Civil Engineering & Energy Technology

Section of Civil Engineering

Master Program in Structural Engineering & Building Technology

MASTER THESIS

TITLE OF REPORT	DATE: 25.05.2023
Abaqus FEA with Concrete Damaged Plasticity and its feasibility in recreating laboratory experiments: A numerical analysis and sensitivity study	PAGES / APPENDICES: 60 / 7
AUTHORS Sander Fagerhøi Anders Kvåle Bergsbakken	SUPERVISOR: Professor Gro Markeset

SUMMARY / SYNOPSIS

A numerical analysis and sensitivity study of Concrete Damaged Plasticity (CDP) in Abaqus FEA, which aims to discover how the base parameters of the plasticity model CDP impacts simulations of concrete cylinders under uniaxial compression and reinforced concrete beams under 4-point bending.

The thesis identifies to which degree different parameters changes simulated behaviour, as well as challenges, shortcomings and possible optimisation opportunities related to future work of this kind.

KEYWORDS
Abaqus FEA
Concrete Damaged Plasticity
Non-linear analysis
Parameter sensitivity analysis

Abstract

Non-linear Finite Element Analysis of concrete is a subject that is constantly worked on. Due to the complex nature of concrete, both in pure states and when reinforced, there are many different models and approaches when it comes to representing the material digitally. A range of systems exist with an even greater range of different theoretical models implemented in an attempt to replicate, predict, and analyse the behaviour of concrete structures.

One such piece of software is Abaqus FEA, which has the concrete model Concrete Damaged Plasticity as part of its base package. This plasticity model is widely used in order to model concrete, and like other material models it requires a range of different material input parameters to be defined correctly – otherwise accurate results cannot be expected to be achieved.

This thesis aims to investigate the material parameter inputs required by Concrete Damaged Plasticity in Abaqus FEA, utilising material data taken from a previously completed experiment which presents its findings in a doctorate, performed and written by Professor Gro Markeset.

By extracting data from Markeset's research, adjusting it according to Concrete Damaged Plasticity theory, and carefully investigating the impact of changing each base parameter, the authors have made an attempt at identifying the parameter values that allows for recreation of the laboratory experiment in the Finite Element Software.

Following this, the thesis looks at the feasibility of extracting the identified parameters and combining them with uniaxial stress-strain data in order to mimic an experimental 4-point bending test of reinforced concrete beams. The research performed by the authors of this thesis covers a wide field of necessary considerations related to this type of work. Lastly, suggestions on how to further this work and increase both accuracy and potential are presented.

Acknowledgements

Firstly, we would like to express our sincere gratitude to our advisor Professor Gro Markeset for her continued support and extensive knowledge about concrete theory. The guidance provided by Markeset has been of great service to the implementation and work conducted in this thesis – not only by providing the groundwork for this thesis, but in particular with the expertise regarding concrete behaviour.

We would like to extend this gratitude to our fellow students of which we have had the pleasure of working with throughout the master's programme. Valuable friendships and acquaintances have been made, and we look forward to seeing them all succeed.

A thanks is in place to the professors of the Department of Built Environment, and the Faculty of Technology, Art and Design.

Five years of Engineering studies are concluded with this thesis. It shall be interesting to get to apply the knowledge gained in our professional careers.

Oslo, 25.05.2023

X Sander Fagerhøi

Sander Fagerhøi

X

Anders Kvåle Bergsbakken

Contents

List of Figures

List of Tables

List of Abbreviations

Abbreviation (alphabetically)	**Definition**
BCM	Brittle Cracking Model
CDP	Concrete Damage(d) Plasticity
CM	Compressive Meridian
DEM	Discrete Element Method
FEA	Finite Element Analysis
FEM	Finite Element Modelling
LFEA	Linear Finite Element Analysis
MC	Mohr-Coulomb (- Failure Criterion)
NLFEA	Non-linear Finite Element Analysis
SCA	Smeared Crack Approach
SCM	Smeared Crack Model
TM	Tensile Meridian

1. Introduction

Non-linear analysis of concrete is a complex process. The material keeps hard-to-predict qualities that can be difficult to replicate and has inspired a range of different models to be used for Finite Element Analysis (FEA, sometimes *slightly incorrectly* referred to as FE Modelling – FEM). In essence, concrete has a stress-strain relation that is considered totally non-linear in compression while tensile capacity is considered marginal. [1] Due to the complex behaviour of concrete under loading, it is necessary to carefully consider which material model to utilise to accurately simulate realistic responses. The need for these models is due to how different concrete may behave under different load conditions, like load type and -speed. [2]

1.1. Goal of thesis

This thesis aims to investigate the Abaqus FEA software's response to the use of Concrete Damaged Plasticity (CDP), one of the available plasticity theories for concrete materials. Utilising data from Professor Gro Markeset and her doctorate [3] on compressive strain gradients for concrete failure, the authors have attempted to recreate – in the FEA software – the responses that was observed in the doctorate. While many parameters of CDP have a set of standard recommended values and one could assume straight forward application, the actual scenario is less simple: many properties of the model are necessary to determine on a case-by-case basis as there is no set consensus for the use of these parameters. [4]

1.2. Research questions

In an attempt to determine the parameter values of the CDP model, a sensitivity study is conducted by modelling a concrete cylinder of three different concrete strengths subjected to a monotonic load case, followed by subjecting a reinforced concrete (RC) beam to an inverted 4-point bending scenario, as depicted in Markeset's experimental work, [3]. The research question that the authors of this work aim to investigate is:

"To which extent is it possible to extract the data from an experimental study on uniaxial concrete compressive testing, recreating the test cylinders as finite element models in Abaqus FEA and simulate the results using Concrete Damaged Plasticity? Will the laboratory results let themselves replicate digitally, and what are the challenges that may prevent the analyses from being as accurate as desired?"

Additionally, it was of the authors' interest to study the following questions:

"How representative are the results from running a non-linear finite element analysis of an over-reinforced concrete beam subjected to 4-point bending, using the values for uniaxial compressive material tests and the results of uniaxial cylinder compressive tests?"

"To which degree can the parameter values that are determined in the sensitivity study of the cylinder tests be transferred to the beam-problem?"

"What are the challenges when attempting to translate uniaxial compressive test values to a beam bending problem? Will the presence of gradient strains and the phenomena of localisation in an over-reinforced concrete beam be a problem for the Concrete Damaged Plasticity model in Abaqus FEA?"

1.3. Thesis structure

This study follows a structure in order to carefully navigate the various challenges that this type of model presents. The theoretical background of CDP is extensive and complicated, not to mention the different settings and optimisation needs in the Abaqus FEA software itself. It is worth noting that various limitations are required to be set in order to set a realistic border within the research is conducted, due to the highly broad potential this type of work offers.

The structure of the presented work can be outlined by the following:

- A theoretical introduction to (non-) linear analysis, material- and finite element modelling, as well as a brief presentation of Abaqus FEA as a commercial modelling software.
- A deep-dive into CDP as a theoretical model within Abaqus, establishing the theory that the simulations are based on. This includes, but is not limited to, the necessary parameter values that the CDP model so heavily rely on.
- Experiences from previous work on the model in the shape of a limited pre-study of a lower strength concrete cylinder.
- A brief literature study to clarify and illustrate the broad difference in findings when it comes to optimal parameter settings and CDP use, and why this detail matter.
- Presenting the modelling procedure to recreate the cylinder and beam specimens from the doctorate [3], addressing any discrepancies between the physical shape of the experiments and the models, and showcasing the settings of the software that are used.
- Displaying the results of the analyses, mainly by way of graphs and general data taken from Abaqus/Explicit.
- A discussion of the results, addressing discrepancies in behaviour between the experimental and Abaqus data sets.
- A conclusive chapter to outline the presented results and discussion, with the authors' own remarks regarding the work and the possibility of further investigation into the matter.

It is worth noting that there are many ways of going forward with this type of problem, and this is just one way the authors consider reliable in order to investigate the sensitivity of the CDP model.

1.4. Thesis limitations

Due to the nature of numerical modelling and non-linear analysis, it is necessary to set some boundaries ahead of the work that the authors of this thesis wish to conduct. Some limitations relate to the FEA software and CDP, and other limitations are tied to available data and time-constraints.

- To begin with, only a limited study of the reinforced concrete beams is conducted due to time constraints and hardware limitations. Due to the amount of time the cylinder tests took, the amount of testing time available for the RC beam analyses was limited.
- Certain sacrifices in simulation accuracy have been made due to limitations in available hardware to run the Abaqus software. The authors are limited to an academic license of Abaqus FEA on their personal hardware, and as such are limited by the computing power that the PCs have.
- With limited source data to utilise for the CDP model, certain assumptions have been made in order to allow for the different analyses to run. In particular, a lack of tensile input data and certain damage model parameters have been determined either theoretically or by collecting tabular data from similar studies.

2. Theory

2.1. Linear analysis: The basics

Model analysis can typically be split into two categories: Linear and non-linear. While linear analysis is a simpler approach to a problem, non-linear analysis is often required for increased accuracy. A linear analysis use force/displacement relationships [5], which depend on some simple assumptions like (for example) strictly elastic behaviour and only considering a single state of stress or applied force at a time. A linear approach allows for simplicity and is *generally* not the most considered condition in regard to real life situations and complex structure behaviour.

Linear analysis is the easiest and least resource consuming method, since finite element solutions only need to be determined using linear sets of equations, and also allows for the application of *superposition*. [6] The trade-off by using linear finite element analysis (LFEA) is that behaviour other than that which is elastic, cannot and will not be considered. This, in turn, means that for problems where there is an expectation of beyond-elastic yielding and plastic properties, non-linear finite element analysis (NLFEA) will have to be considered. Figure 1 illustrates a simplistic approach to linear analysis, courtesy of [7].

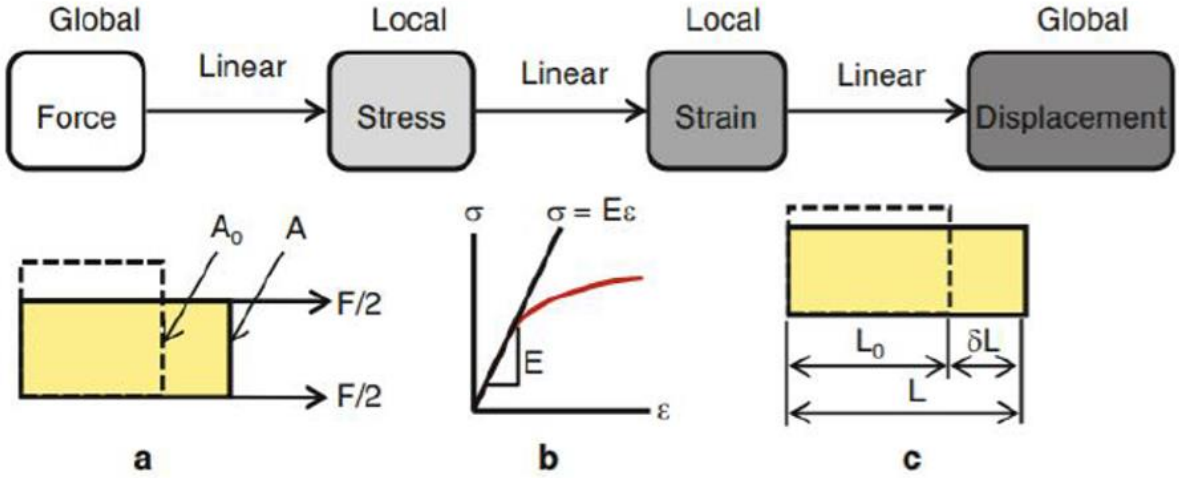

Figure 1: Linear approach illustrated. Courtesy of [7].

2.2. Non-linear analysis

Non-linear analysis is a different story. Simply put, non-linearity is defined as anything not linear [7, 8], and nearly all practically applied systems include one form of non-linear behaviour or another. In relation to structural mechanics, phenomena like material yielding, creep, buckling and gap formations can be difficult to describe accurately, and require complicated numerical models and equations. [8]

Nonlinear phenomena can be split into various categories – including but not limited to:

- Material nonlinearity:
  - Elasticity, plasticity, and creep described by stress and/or strain.
- Contact nonlinearity:
  - Sliding contact, impact, and gap changes.
- Geometric nonlinearity:
  - Deformations becoming large enough to require consideration of the deformed structure in equilibrium equations.

While the principle of superposition is greatly appreciated in linear problems, this is rendered useless in non-linear problems. In essence, every load case has to be run through its own separate analysis, and there may be more than a single solution to a set of loads depending on the application of the load sequences. [8]

Figure 2 illustrates how the dynamics of an analysis changes when the problem turns from a linear to a non-linear one.

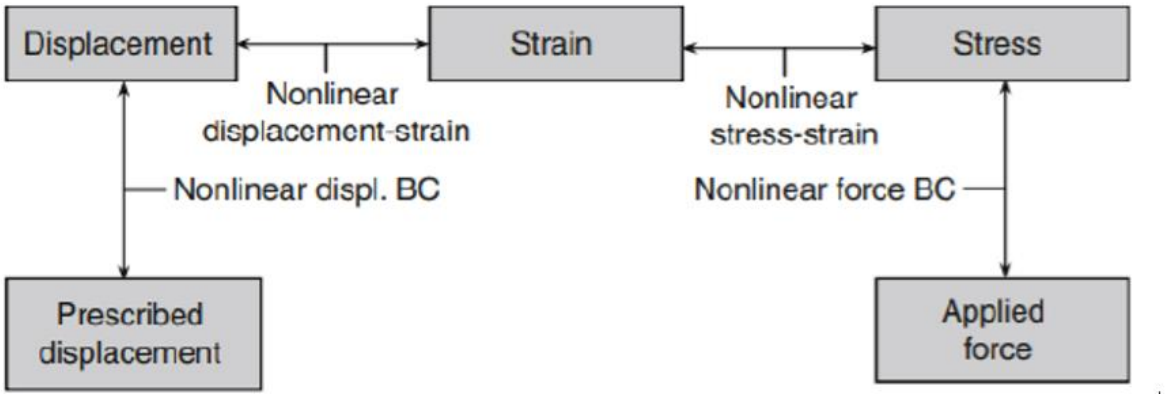

Figure 2: Non-linear analysis illustrated. [7]

Non-linear problems have various methods of solution. A few examples of this would be the *Newton-Raphson (NR)* and *Modified* NR methods, direct substitution, the initial stiffness method, or any number of other available models.

2.3. Non-linearity of concrete

The strength of concrete varies vastly. Typically, structural concrete strength classes range from as low as 20-30 MPa (low strength concrete) to as high as 150+ MPa (ultra-high strength concrete), with the utilised strength class depending on different design scenarios. A standard way of testing concrete strength is by way of uniaxial and biaxial compressive testing. An important thing to understand about concrete strength is that as its strength in compression goes up, tensile capacity similarly increases – and this increase in strength has a direct effect on the behaviour of stress-strain curves, [9].

Figure 3 details this effect; As the concrete strength goes up, the material displays increasingly brittle behaviour, where drastic degradation beyond the ultimate yield strength is more and more pronounced. Lower strength concrete types, while having less ultimate strength, portrays more ductile stress-strain relations and less brittle characteristics. It should be noted that, in general, pure concrete is definitely not considered a ductile material but rather can display certain ductile properties. This ductile potential is further enhanced by including various additives in the concrete paste: for instance, metallic and polymeric fibres or different types of admixtures.

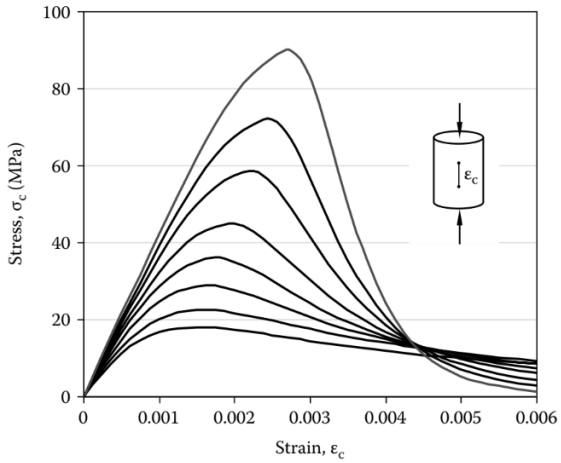

Figure 3: Variation of concrete stress-strain curves under uniaxial compression depending on strength of concrete specimen. [9]

For this study, a set of curves are provided by Markeset from the laboratory [3] which depict a somewhat similar behaviour, see Figure 4, taken from a series of cylinder compression tests. ND25, ND55 and ND90 denote concrete strength classes that has been considered for this thesis, where ND25 is the weakest of the types and ND90 is the strongest. LWA60 is a light-weight aggregate concrete similar to Light Clay Aggregate concrete (e.g., LECA). The LWA60 test has not been considered in this thesis, due to the lack of actual data to use.

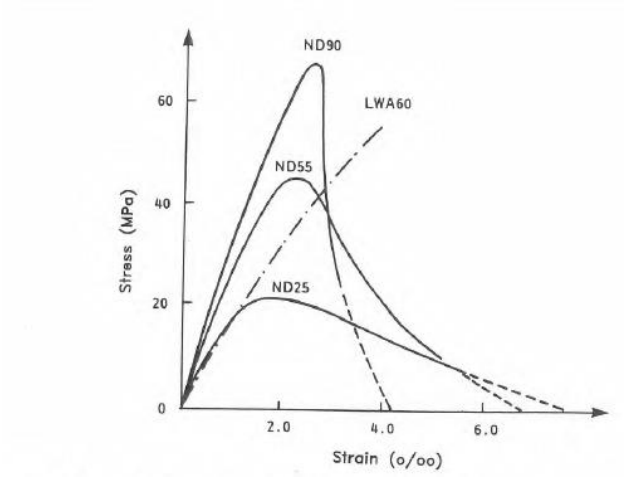

Figure 4: Stress-Strain sample curves from Professor Markeset's laboratory work. [3].

As can be observed, similarities between Figure 3 and Figure 4 are present with increasing brittleness following the increasing concrete strength. A post-yielding phase is recorded in the experiments, until discontinuation of said data recording due to the setup, and then a dotted, extrapolated line represents the *expected* continuation of the stress-strain recording. To which extent these curves are possible to recreate in Abaqus FEA using CDP is what the authors wish to investigate.

2.4. Finite Element Modelling of concrete

2.4.1. Some material behaviour theories

With concrete, strength in compression versus tension is known to be vastly different: the former being significantly higher than the latter – it is additionally important to note that concrete's tensile stress-strain relations are considered primarily near-linear. This is not the case for its capacities and behaviour in compression, which is considered to be entirely non-linear. [10] Multiple equations and models try to describe this plastic behaviour in various ways, which include models like the Mohr-Coulomb failure criterion [11-13], the Drucker-Prager criterion [14], and the Von Mises model [15]. These are only a few of many models which are used for a variety of materials; Drucker-Prager in particular is relevant due to its use to define CDP rules in Abaqus FEA – as described in the manuals. [16-18]

The Von Mises yield criterion (*or -theory*) is a criterion primarily designed for *ductile materials*, for instance many types of metals. This theory explains how ductile material yield occurs when the second invariant of deviatoric stress (J_2) reaches a critical limit, and the simplest mathematical definition of the theory is expressed by [15]:

$$J_2 = K^2 \qquad \textit{Eq. 1}$$

where $K = \frac{\sigma_y}{\sqrt{3}}$ = material yield stress in pure shear, and σ_y = material yield strength in tension.

Another common way of describing Von Mises yield, is by way of the principal stresses:

$$\sqrt{\frac{1}{2}[(\sigma_1 - \sigma_2)^2 + (\sigma_2 - \sigma_3)^2 + (\sigma_3 - \sigma_1)^2]} = \sigma_y \qquad \textit{Eq. 2}$$

The left part of the equation is also referred to as the *Mises equivalent stress*, utilised in FEA software to express (risk of) yield and failure – including Abaqus FEA.

For brittle material scenarios, other theories are more relevant to consider. The Mohr-Coulomb failure criterion (*MC*) is a model based on "*a set of linear equations in principal stress space describing the conditions for which an isotropic material will fail (…)*" [11], and can be written as a function in two distinct ways: of major principal stress, σ_I, and minor principal stress, σ_{III}, *or* of normal stress, σ, and shear stress, τ, on the failure plane. MC is known to be reasonably applicable in scenarios of pure-compressive stresses to rock and draws its advantage in use from its mathematical simplicity with relatively clear parameter definitions [11].

The Drucker-Prager criterion is the most relevant theory for this thesis. This criterion has been modified by Lubliner et al. [19] and Lee & Fenves [20] for the specific use in CDP, and it is described as a "*three-dimensional pressure dependent model to estimate the stress state at which the rock reaches its ultimate strength*" [21]. The theory is considered a generalisation of the MC theory, and the expression for this criterion can be written as

$$\sqrt{J_2} = \lambda I_1 + \kappa \qquad \textit{Eq. 3}$$

where λ and κ = material constants, while $I_1 = \sigma_1' + \sigma_2' + \sigma_3' =$ first invariant of the stress tensor. σ_{1-3}' are the principal effective stress values.

2.4.2. Difficulties of modelling heterogenous materials

Non-linear behaviour of concrete is characterised by changes in the response (i.e., stress and deformations) which are not proportional to the applied loads, in turn induced by the complex and varied microstructure that forms when creating concrete from aggregates, cement, and water. This non-linearity is typically manifested in different ways like strength degrading, crack formations and inelastic deformations. These responses are naturally dependent on factors like the concrete composition, rate of loading, load- and support conditions. [2, 22] This variation in behaviour is largely the reason why concrete is such a difficult material to accurately simulate and explains why currently no consensus on a material model is set: The *heterogeneous* nature of concrete is *hard to predict*.

While fairly accurate recreation of the meso-structure of concrete is certainly doable and could allow for advanced modelling scenarios – for instance by utilising the Discrete Element Method (*DEM*) [23], completely accurate and exact modelling of the heterogeneous nature of concrete would require an immense amount of computational power [23, 24], in turn increasing time required for simulations: It quickly becomes impractical to go to these levels of detail unless the purpose of doing so explicitly requires it, e.g. due to very specific design needs. Figure 5 is an example that shows why meso-structure simulations are prone to become expensive in regard to computing and time: thousands of clusters are created, and then all contact between the three-element clusters must be registered and bonded to create the superstructure. The intent is to add a degree of randomness to the model, simulating the random orientation and placement of aggregates and potential fibres in real-life concrete – and this comes at computational cost. Courtesy of F.A. Tavarez and M. E. Plesha [23]

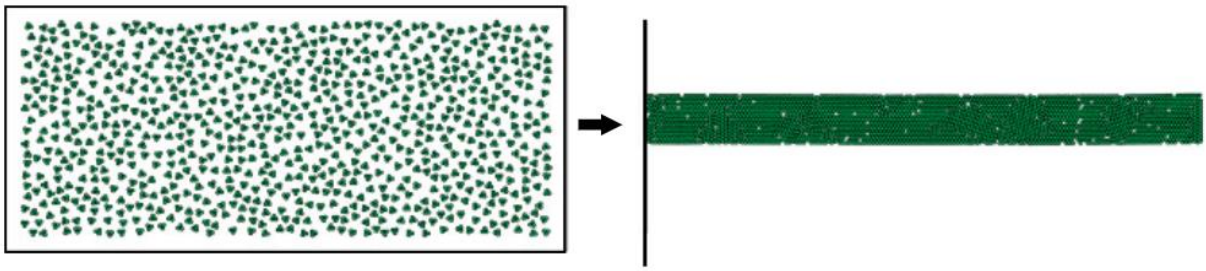

Figure 5: Example of a DEM cantilever model, visualising the time-consuming and highly detailed process of meso-scale modelling. Courtesy of [23].

The challenges of modelling the meso-structure of concrete is the reason why, in many general applications, concrete is created while assuming that it is a homogeneous (macro-scale) material. [24] This is the case for all of the concrete models that are available in the Abaqus FEA package that the authors have access to.

2.5. Smeared crack approach in Abaqus FEA

Abaqus FEA allows for a few different approaches when modelling concrete; Three primary models are provided unless one decides to utilise original, specialised code for specialty cases. Two of these models use the *Smeared Crack Approach* (*SCA*), and all models are described in the publicly available Abaqus manuals, [16-18]. These manuals are the basis for the next chapters discussing the Abaqus FEA concrete models, chapters 2.5 and 2.6.

2.5.1. Smeared Crack Model (SCM)

The Smeared Crack Model is an inelastic constitutive model intended for use in Abaqus/Standard. SCM is primarily intended for observing concrete behaviour under monotonic and low confining pressure. The model does not support modelling of effects related to reinforced concrete, such as bond slipping and dowel behaviour – unless the plain concrete is given some artificial characteristics, for instance through the use of *tension stiffening*, in order to mimic this type of behaviour. The model is not intended for cyclic loading cases, nor is it meant to simulate the reduction of elastic stiffness that is caused by inelastic strains.

2.5.2. Brittle Cracking Model (BCM)

The Brittle Cracking Model is a cracking constitutive model available to use in *Abaqus/Explicit*. Similar to SCM, BCM must be given artificial parameter values to simulate reinforcement-concrete behaviour. In relation to concrete behaviour, BCM is only intended for the brittle aspects of concrete that occur during tensile and tensile-compressive load cases: cleavage, shear and mixed mode fracturing are among the observed mechanisms in this scenario. Thus, ductile behaviour/tendencies of concrete that occur from compressive stress states are unfit to be simulated with BCM.

2.6. Concrete Damaged Plasticity

The third available approach in Abaqus FEA is the Concrete Damaged Plasticity model. CDP is derived from the Drucker-Prager criterion [14], with modifications later introduced by Lubliner et al. [19] as well as an additional revision performed by Lee and Fenves [20]. CDP is described as model based on scalar plastic damage theory [16-18]. The purpose of the model is to analyse concrete's plastic behaviour, which includes the post-peak softening and damage patterns, specifically by running a range of analyses in Abaqus/Explicit.

The Simulia Abaqus manuals [16-18] provided by Dassault Systèmes describes the theory of the model in a clear manner. CDP is referred to as an "incremental" theory, which is formulated by three key terms:

- *Yield surface*: a generalisation of what is considered a "yield load", which tests the material response for pure elastic behaviour at certain stress states.
- *Flow rule*: a definition of inelastic deformation occurring when the material stops behaving purely elastically.
- *Hardening rules*: defining how the former two properties change as inelastic deformations occur.

The following chapter discuss the theory of CDP as described by the manuals and use these manuals heavily to describe the theory in a condensed way i.e., the manuals are the source of chapter 2.6. The purpose of the chapter is to form a condensed overview of the processes that happen behind the scenes when the software runs the Concrete Damaged Plasticity model. For clear transparency with chapter 2.6: Any information taken from any other source than the Abaqus manuals, [16-18], will be listed where it is relevant to do so. Any and all other information presented in this chapter stems from [16-18].

To begin with an additive *Strain Rate Decomposition* is considered:

$$\dot{\varepsilon} = \dot{\varepsilon}^{el} + \dot{\varepsilon}^{pl} \qquad \textit{Eq. 4}$$

$\dot{\varepsilon} =$ total strain rate

$\dot{\varepsilon}^{el} =$ elastic strain rate

$\dot{\varepsilon}^{pl} =$ plastic strain rate

Meanwhile, the *stress-strain relation* in CDP is defined by *scalar damaged plasticity*:

$$\sigma = (1-d)D_0^{el} : (\varepsilon - \varepsilon^{pl}) = D^{el} : (\varepsilon - \varepsilon^{pl}) \qquad \textit{Eq. 5}$$

This means that the failure mechanisms associated with damage of concrete leads to a reduction in the elastic stiffness.

$D_0^{el} =$ initial (or undamaged) elastic stiffness

$D^{el} = (1-d)D_0^{el} =$ degraded elastic stiffness; governed by the scalar stiffness degradation variable *d*. The variable, *d*, is discussed further in chapter 2.6.9 Damage Parameter**.**

Briefly put: $(1-d)$ is an expression of how much of the area is still load-bearing (as opposed to damaged), with no damage corresponding to a value of $d = 0$ and total damage where $d = 1$.

2.6.1. Flow Rule

The flow rule of the model determine how plastic flow is handled. It is closely related to the plastic strain rate tensor, $\dot{\varepsilon}^{pl}$, by the expression:

$$\dot{\varepsilon}^{pl} = \dot{\lambda}\frac{\partial G(\bar{\sigma})}{\partial \bar{\sigma}} \qquad \textit{Eq. 6}$$

which is governed by $G = \textit{flow potential}$. $\dot{\lambda}$ is a *positive* (read: cannot be less than 0) plastic multiplier. In CDP, the flow potential is expressed as a Drucker-Pager hyperbolic function:

$$G = \sqrt{(\epsilon \cdot \sigma_{t0} \cdot tan\varphi)^2 + \bar{q}^2} - \bar{p} \cdot tan\varphi \quad \textit{Eq. 7}$$

$\epsilon(\theta, f_i) =$ *flow potential eccentricity*, described in sub-chapter 2.6.5 Flow Potential Eccentricity**.**

$\sigma_{t0}(\theta, f_i) =$ uniaxial tensile stress at failure. This is defined by the user, as *tension stiffening*.

$\varphi(\theta, f_i) =$ is the dilation angle. Measured at high confining pressures, this angle is in relation to the *p-q/t* (meridian-) plane. More about this in 0 Dilation Angle.

2.6.2. Hardening

In the concrete model, microcracks and crushing are defined using *hardening variables*, which control how the yield surface evolves and how the elastic stiffness degrades – as well as being closely related to dissipated *fracture energy*, G_f.

The tensile equivalent plastic strain, $\tilde{\varepsilon}_t^{pl}$; and the compressive equivalent plastic strain, $\tilde{\varepsilon}_c^{pl}$, are evolved using the expression:

$$\tilde{\varepsilon}^{pl} = \begin{bmatrix} \tilde{\varepsilon}_t^{pl} \\ \tilde{\varepsilon}_c^{pl} \end{bmatrix} ; \; \dot{\tilde{\varepsilon}}^{pl} = h(\bar{\sigma}, \tilde{\varepsilon}^{pl}) \cdot \dot{\varepsilon}^{pl} \quad \textit{Eq. 8}$$

$\dot{\tilde{\varepsilon}}^{pl} =$ equivalent plastic strain rate

$\dot{\varepsilon}^{pl} =$ plastic strain rate tensor.

2.6.3. Yield Surface

The yield surface of CDP is governed by a *yield function*, which determines the state of damage and/or failure. This function is a representation of a surface in the effective stress space submitted to damage. It is defined using:

$$F(\bar{\sigma}, \tilde{\varepsilon}^{pl})$$

$\bar{\sigma} =$ effective (uniaxial) cohesion stress, which is used to determine the size of the yield surface(s). This cohesion value is expressed by:

$$\bar{\sigma}_{t/c} = \frac{\sigma_{t/c}}{(1 - d_{t/c})} = E_0(\varepsilon_{t/c} - \tilde{\varepsilon}_{t/c}^{pl}) \quad \textit{Eq. 9}$$

**the subscript t/c refers to whether tensile or compressive cohesion stress is calculated, and they are calculated separately in their own expressions – the expressions are compressed to a single one here for simplicity.*

The yield function, $F(\bar{\boldsymbol{\sigma}}, \tilde{\boldsymbol{\varepsilon}}^{pl})$, is used in CDP to express a *yield condition*. The yield function originates from Lubliner et al.[19] , with the later addition from Lee and Fenves [20], in order to allow for the difference in strength evolution that is observed under tensile and compressive loading. The shape of the yield function is:

$$F(\bar{\boldsymbol{\sigma}}, \tilde{\boldsymbol{\varepsilon}}^{pl}) = \frac{1}{1-\alpha}(\bar{q} - 3\alpha\bar{p} + \beta(\tilde{\boldsymbol{\varepsilon}}^{pl})\langle\hat{\bar{\sigma}}_{max}\rangle - \gamma\langle-\hat{\bar{\sigma}}_{max}\rangle) - \bar{\sigma}_c(\tilde{\varepsilon}_c^{pl}) \leq 0 \qquad \textit{Eq. 10}$$

$\alpha, \gamma =$ material constants

$\bar{p} = -\frac{1}{3}\bar{\sigma} : \mathbf{I} =$ effective hydrostatic pressure

$\bar{q} = \sqrt{\frac{3}{2}\bar{S} : \bar{S}} =$ Mises equivalent effective stress

$\bar{S} = \bar{p}\mathbf{I} + \bar{\sigma} =$ deviatoric part of the effective stress tensor $\bar{\boldsymbol{\sigma}}$. $\hat{\bar{\sigma}}_{max}$ is the algebraical maximum of the eigenvalue of $\bar{\boldsymbol{\sigma}}$.

The function for β is given by:

$$\beta(\tilde{\boldsymbol{\varepsilon}}^{pl}) = \frac{\bar{\sigma}_c(\tilde{\varepsilon}_c^{pl})}{\bar{\sigma}_t(\tilde{\varepsilon}_t^{pl})}(1-\alpha) - (1+\alpha) \qquad \textit{Eq. 11}$$

In the case of biaxial compression where $\hat{\bar{\sigma}}_{max} = 0$, the yield function $F(\bar{\boldsymbol{\sigma}}, \tilde{\boldsymbol{\varepsilon}}^{pl})$ will be reduced to the *Drucker-Prager criterion.*

It is possible to express the material constant α by means of initial (equi-)biaxial compressive yield stress, σ_{b0}; and uniaxial compressive yield stress, σ_{c0};

$$\alpha = \frac{\sigma_{b0} - \sigma_{c0}}{2\sigma_{b0} - \sigma_{c0}} \qquad \textit{Eq. 12A}$$

The ratio between these two yield stress values, σ_{b0} and σ_{c0}, is utilised as a modelling parameter directly in Abaqus FEA – denoted as *fb0/fc0* in the software – when defining material properties: See chapter 2.6.6 fb0/fc0. To specify how the ratio σ_{b0}/σ_{c0} relates to α, the expression can be expanded:

$$\alpha = \frac{(\sigma_{b0}/\sigma_{c0}) - 1}{2 \cdot (\sigma_{b0}/\sigma_{c0}) - 1} \qquad \textit{Eq. 12B}$$

*This expanded form is often used in other literature describing this ratio.

A necessary condition for this material constant is $0 \leq \alpha \leq 0.5$. Any attempts at exceeding these limit values will be negated by Abaqus FEA automatically defaulting to the closest limit value.

Finally, the constant γ is possible to express in a simple function:

$$\gamma = \frac{3(1 - K_c)}{2K_c - 1} \qquad \textit{Eq. 13}$$

K_c is another modelling parameter that is used as input in material properties: the ratio of the second stress invariant on the *tensile meridian (TM)*, $\bar{q}_{TM}$; to the second stress invariant on the *compressive meridian (CM)*, $\bar{q}_{CM}$; at initial yield – also see sub-chapter 2.6.7 K_c.

A necessary condition for this ratio is that a pressure invariant, p, has a value which yields negative maximum values of principal stress: $\hat{\sigma}_{max} < 0$.

For the TM to become a valid expression, the stress states need to satisfy the condition:

$$\hat{\bar{\sigma}}_{max} = \hat{\bar{\sigma}}_1 > \hat{\bar{\sigma}}_2 = \hat{\bar{\sigma}}_3 \qquad \textit{Eq. 14}$$

while for the CM, the stress states follow the condition:

$$\hat{\bar{\sigma}}_{max} = \hat{\bar{\sigma}}_1 = \hat{\bar{\sigma}}_2 > \hat{\bar{\sigma}}_3 \qquad \textit{Eq. 15}$$

$\hat{\bar{\sigma}}_{1-3}$ are effective stress tensor ($\bar{\boldsymbol{\sigma}}$) eigenvalues. The maximum eigenvalue $\hat{\bar{\sigma}}_{max}$ for the TM and the CM is:

$$(\hat{\bar{\sigma}}_{max})_{TM} = \frac{2}{3}\bar{q} - \bar{p} \qquad \textit{Eq. 16}$$

$$(\hat{\bar{\sigma}}_{max})_{CM} = \frac{1}{3}\bar{q} - \bar{p} \qquad \textit{Eq. 17}$$

When $\hat{\bar{\sigma}}_{max} < 0$, this will result in the following yield conditions:

$$TM\text{: } \left(\frac{2}{3}\gamma + 1\right)\bar{q} - (\gamma + 3\alpha)\bar{p} = (1 - \alpha)\bar{\sigma}_c \qquad \textit{Eq. 18}$$

$$CM\text{: } \left(\frac{1}{3}\gamma + 1\right)\bar{q} - (\gamma + 3\alpha)\bar{p} = (1 - \alpha)\bar{\sigma}_c \qquad \textit{Eq. 19}$$

When $\hat{\bar{\sigma}}_{max} > 0$, the yield conditions become:

$$TM: \left(\frac{2}{3}\beta + 1\right)\bar{q} - (\beta + 3\alpha)\bar{p} = (1-\alpha)\bar{\sigma}_c \qquad \textit{Eq. 20}$$

$$CM: \left(\frac{1}{3}\beta + 1\right)\bar{q} - (\beta + 3\alpha)\bar{p} = (1-\alpha)\bar{\sigma}_c \qquad \textit{Eq. 21}$$

The *yield surface*, following these conditions, is illustrated in two ways. The *deviatoric plane* yield surface, orthogonal to the hydrostatic axis, takes the shape of the left side of Figure 6. If regarded in plane stress, the right side illustrates the yield surface for both uniaxial and biaxial stress conditions.

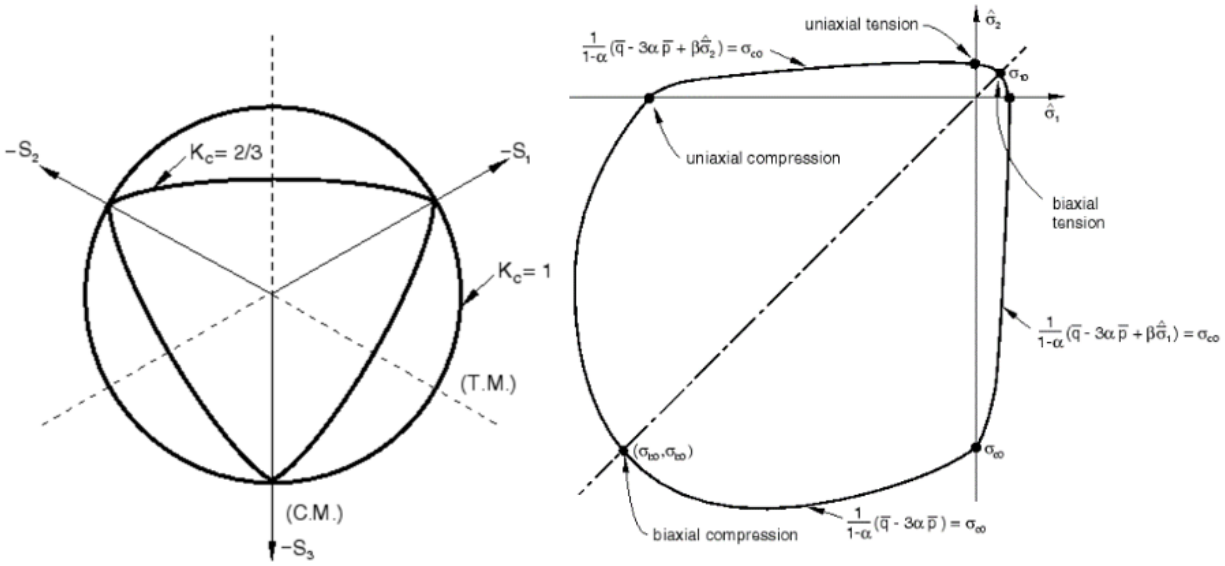

Figure 6: Yield surfaces in the deviatoric plane (left) and for in-plane stress (right) courtesy of the User's guide [16]

2.6.4. Dilation angle

The dilation angle (in some studies referred to as *dilatation angle*) is an important parameter of the CDP model. This parameter describes the internal friction angle of the concrete, or can more specifically be determined using the ratio of volumetric change over axial strain [25]:

$$\psi = \arcsin\left(\frac{\frac{\delta e_v}{\delta e_a}}{\frac{\delta e_v}{\delta e_a} - 2}\right) \qquad \textit{Eq. 22}$$

The general recommendations regarding dilation angles float from 30 to 40 degrees, and almost any change to this value will have an impact on the simulations that are run.

The geometric relevancy of the dilation angle can be showcased using the Hyperbolic Drucker-Prager flow potential, see Figure 7 [26].

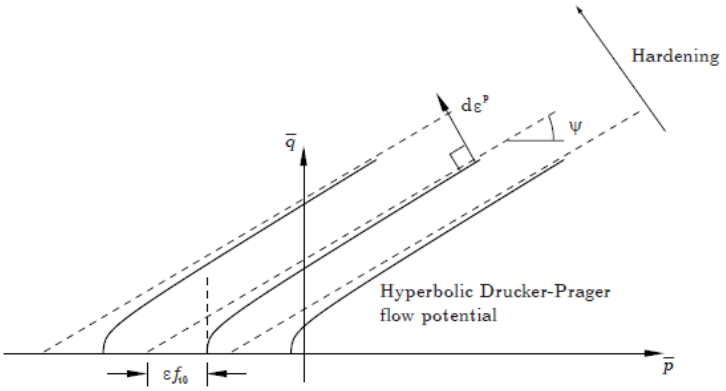

Figure 7: Hyperbolic Drucker-Prager potential [26].

2.6.5. Flow potential eccentricity

The flow potential eccentricity, ϵ, is defined as the rate the flow potential function reaches the asymptote of the user-defined dilation angle ψ. In general, the flow potential will trend toward a straight line as the eccentricity approaches a value of 0, defining the *linear Drucker-Prager yield criterion*, while increasing the value of ϵ will increase the curvature of the flow potential. Figure 7 also shows the geometric meaning of the eccentricity in the meridional plane.

2.6.6. fb0/fc0

The ratio of initial equibiaxial compressive yield stress to initial uniaxial compressive yield stress – σ_{b0}/σ_{c0} or *fb0/fc0* – relates to the expansion of the cylinder when submitted to uniaxial compression. The default value in Abaqus FEA is set to 1.16, and while changing this value will cause some changes to the behaviour of the concrete it is highly unlikely that a value below 1 would cause realistic values. A ratio less than 1 would imply the concrete cross section would *shrink* under compressive stress; highly counterintuitive and naturally not realistic. The ratio is possible to consider using the side of Figure 6 for the in-plane stress

yield surface for concrete under biaxial stresses. The yield function, *F*, also has a dependency on the maximum principal stresses which is illustrated in this figure. With tension in the stress tensor, maximum stress becomes positive which in turn yields a non-zero value for β. Meanwhile, γ is not represented in this figure as this material constant relates to triaxial compression.

2.6.7. Kc

The parameter K_c, the *ratio of the second stress invariant on the tensile meridian to that on the compressive meridian ($\bar{q}_{TM}/\bar{q}_{CM}$)* (also see chapter Yield Surface), has a limitation in regard to its values. It *must* satisfy the rule $0.5 < Kc < 1.0$, in which a value of 2/3 is the recommended/agreed-upon standard. The yield surfaces of the deviatoric plane shows how the value of K_c may vary and how this affects the function, see the left side of Figure 6.

An important note to make about K_c is that this value is related to the dilation angle and the eccentricity, and a change to one will often require a change in all three parameters – but not always.

2.6.8. Viscosity

The viscosity parameter works as a representation of the relaxation time of the viscoplastic system. The value finds it use as a part of the Duvaut-Lions regularisation [27], which may be found necessary if the softening behaviour and stiffening degradation of the model leads to convergence problems. Viscoplasticity allows stresses of the model to go beyond the limits of the yield surface. The Duvaut-Lions equation can be expressed through:

$$\dot{\varepsilon}_v^{pl} = \frac{1}{\mu}(\varepsilon^{pl} - \varepsilon_v^{pl}) \qquad \textit{Eq. 23}$$

$\dot{\varepsilon}_v^{pl} =$ viscoplastic strain rate tensor

$\mu =$ Viscosity parameter

$\varepsilon^{pl} =$ plastic strain in the inviscid backbone model

The viscosity parameter, μ, is also implemented in an expression for the viscous stiffness degradation variable:

$$\dot{d}_v = \frac{1}{\mu}(d - d_v) \qquad \textit{Eq. 24}$$

$d =$ degradation variable in the inviscid backbone model

$d_v =$ viscous stiffness degradation variable

The overall stress-strain relationship in the viscoplastic model scenario is given as:

$$\sigma = (1 - d_v) D_0^{el} : (\varepsilon - \varepsilon_v^{pl}) \qquad \textit{Eq. 25}$$

In essence, in relation to time, the viscosity parameter will allow for a model with convergence issues to improve its softening regime, usually without this impacting results severely – as long as the values of viscosity parameter are *small* in comparison to the given time increments, and only *if the model struggles with convergence*. A value of *0.0001* for this parameter is generally considered adequate and should rarely be set higher. A value of 0 means no viscoplastic regularisation will occur. If the value of this parameter is set too high, unrealistic stiffness may occur in the model. [28]

2.6.9. Damage parameter

The damage parameters that are used in CDP are simple to explain, but they are much more complicated to implement accurately. In essence, concrete will experience micro-cracking when subjected to loading (even at fairly low stresses). This cracking will inevitably lead to a reduction in stiffness which over time can become problematic and is thus relevant to model. The damage parameters in Concrete Damaged Plasticity, also referred to as stiffness reduction factors, are numerical representations of how much stiffness remains in the concrete – the parameters are given as values which range between 0 (no loss in stiffness, no damage) and 1 (total loss of stiffness, full damage). The exact damage values of each concrete type should ideally be calculated with the help of experimental lab results:

$$d_{t/c} = 1 - \frac{E_i}{E_0} \qquad \textit{Eq. 26}$$

By performing ramped loading/unloading cycles, the damage evolution of the concrete can be specified by calculating the evolution of the Young's Modulus. As the degrading E-modulus approaches 0 after cycling the load repetitively, the fraction in Eq. 26 approaches 0 and the total value of *d* approaches 1. Lee & Fenves' curves for cyclic loading [20] shows this degradation of the Young's Modulus accurately.

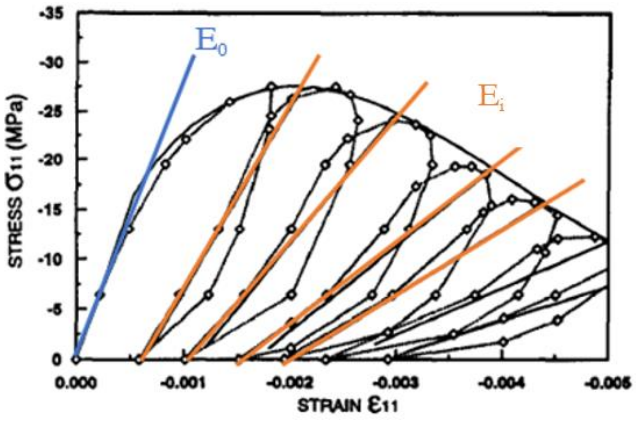

Figure 8: Development of the degrading Young's Modulus, as depicted by Lee & Fenves [20]. Note how E is rapidly reduced as more loading cycles are introduced.

When a lack of experimental results hinders the acquisition of the degraded Young's Modulus, there is a way to *assume* and approximate the damage evolution of the concrete. By recording the crushing stress of the concrete and the following stresses beyond this point during loading, a relation can be created which functions as this approximated damage parameter [20]:

$$d_{t/c} = 1 - \left(\frac{\sigma_i}{\sigma_{cu}}\right) \qquad \textit{Eq. 27}$$

Using this formula for the damage parameter, a tabular array of values is set up where a value of damage will correspond to a value of inelastic strain, ε^{in}:

$$\varepsilon^{in} = \varepsilon_i - \left(\frac{\sigma_i}{E_0}\right) \qquad \textit{Eq. 28}$$

This array will then create the foundation for the damage evolution of the concrete in the CDP model.

The inelastic strain presented in Table 1, calculated using Eq. 28, is controlled using a check for plastic strains. Eq. 30 describes this control equation:

$$\varepsilon^{pl} = \varepsilon^{in} - \left(\frac{d_{t/c}}{(d_{t/c} - 1)}\right) * \left(\frac{\sigma_i}{E_0}\right) \qquad \textit{Eq. 29}$$

This check determines whether or not the inelastic strain and damage parameter values are valid for the model, by ensuring that ε^{pl} remains a positive value and that it does not decrease. If invalid inelastic strain values are used as input for CDP, an error message will alert the user about decreasing and/or negative plastic strain values for the damage evolution of the model.

Stress	Strain	Inelastic strain	Damage parameter	Plastic strain
38.75	0.0013	5.2506E-06	0.461805556	-0.001105728
41.5	0.0014	1.33652E-05	0.423611111	-0.001005728
44	0.0015	2.98329E-05	0.388888889	-0.000905728
46.5	0.0016	4.63007E-05	0.354166667	-0.000805728
48.75	0.0017	7.11217E-05	0.322916667	-0.000705728
60.25	0.0022	0.000186874	0.163194444	-0.000205728
62.25	0.0023	0.000220048	0.135416667	-0.000105728
64.25	0.0024	0.000253222	0.107638889	-5.72792E-06
65.75	0.0025	0.000303103	0.086805556	9.42721E-05
67.25	0.0026	0.000352983	0.065972222	0.000194272
68.5	0.0027	0.000411217	0.048611111	0.000294272
69.75	0.0028	0.000469451	0.03125	0.000394272

Table 1: Plastic strain check, inelastic strain, and damage parameter calculation

The values in Table 1 marked in blue are the input values required for the compressive property definition of CDP in Abaqus FEA – the process is the same for tensile values, but naturally stress values are much lower. Any inelastic strain and damage parameter that yields a negative plastic strain value, cannot be included as an input value for CDP, otherwise the analysis will not run.

2.6.10. Crucial limitations of Abaqus/Explicit and the CDP model

If utilised for pure concrete simulations, the CDP model is heavily mesh-dependent. This means meshing has to be carefully considered and tested in order to ensure the model is as accurate as it possibly can be. The mesh size is also closely related to the time increments of the analyses – something which CDP and Abaqus/Explicit rely heavily on. The model requires properly sized time increments in order to optimise simulation time, and this increment – in the Abaqus manuals referred to as *stable time increment (SI)* – is automatically calculated by Abaqus. The SI relates to the elements of the model, where each element will be checked against a test to determine the lowest *element stable time increment (ESI)*. The lowest available ESI then determines the lowest possible SI of the entire model, [29]. The following equation is used to determine the time increment of the model:

$$\Delta t = \frac{L_e}{\sqrt{\frac{E}{\rho}}} \qquad \textit{Eq. 30}$$

$L_e =$ effective length of element

$E =$ Young's modulus of the element material

$\rho =$ density of element material

The important thing to note with the time increment, is that it is directly related to the overall size of the elements that the model consists of. The optimisation need therefore has its roots in how fine of a mesh one can afford to run, which in turn decides how fine of a time increment can be allowed – a finer mesh model can not only take longer overall to run due to more elements to analyse but also because more steps *can* be taken, while a more coarse mesh will reduce runtime at the cost of increased time steps – which will reduce accuracy: sometimes drastically so.

The remaining parts of the time increment are the Young's modulus (which cannot be edited at free will for the sake of optimisation) and the material density. The density can be tinkered with, as long as the analysis does not aim to include dynamic behaviour. It is, however, sometimes difficult to completely rule out that dynamic behaviour will occur within a model.

Chapter 2.6.9 describes the CDP model's dependency on valid plastic strain values, as shown in Table 1. If the experimental base data used for the calculation of CDP input strains are unusual, running an accurate CDP analysis can prove to be difficult. It is crucial to ensure that the experimental data is checked against the plastic strain requirement from Eq. 29, otherwise the input data simply cannot be trusted to yield analysis results as expected. CDP's plastic strain check tends to be sensitive; should initial attempts at using input data fail, the user may have to compromise parts of the analysis by removing the parts of the inelastic strain data that yields invalid plastic strains.

Similar testing to the one performed in this research can be performed in Abaqus/Standard; however, the authors chose to utilise Explicit solving methods as part of the research that is conducted for this thesis. Explicit solving methods have certain limitations and opportunities that implicit solvers do not, and include (but are not limited to):

- Explicit solvers are more suited for faster events and is more efficient computationally. Due to time- and hardware constraints, the availability of increasing the event-time (and thus, total run-time) is limited. Therefore, running *relatively* fast load sequences (at the absolute fastest, simulations are run with 50mm deformations over 1 second) are a compromise that is taken into consideration for the sake of convenience. This compromised approach is to be considered in the discussion of this thesis.
- Explicit solvers take up less storage space on the hard disk. This ties in with the last point regarding hardware constraints.
- Faster strain rates are more suited to compute using Explicit solvers.
- Time steps can be manipulated using mass scaling (via material density), mesh size and Young's modulus, allowing for increased customisability.

2.7. Fracture energy and strain gradients

An important phenomenon to take into consideration when regarding concrete under stress is fracture energy theory. For tension, CDP defines a fracture energy cracking criterion, G_f, [16-18] based on Hillerborg's fracture energy proposal [30], and is considered adequate for most applications with concrete that experiences tensile stress. However, there is no native definition of the *compressive fracture energy* G_c in CDP.

The need to define a compressive fracture energy is relevant when considering compressive strain gradient theory – in particular for reinforced concrete specimens. As described in Markeset's research, strain gradients have a pronounced effect on a concrete structure's strength and ductility. [3] In the journal article *"On crack band model in finite element analysis of concrete fracture in engineering practise"* [31], a localisation limitation is introduced to limit the amount of ductile response in the material, which can become excessive when the finite elements are made smaller.

Abaqus and CDP lacks a simple approach to strain gradients and localisation. In fact, the steps to allow strain gradients in CDP are complex enough for previous research to attempt simplification, in order to make it easier for the average Abaqus user to accurately account for the effects of compressive strain gradients. For instance, Zhang et al. [32] created a new simplified approach to localisation of strain gradients in Abaqus. By creating a custom user element subroutine (in essence, implementing original code in the backbone code of Abaqus), the authors of *"A simple implementation of localizing gradient damage model in Abaqus"* introduced a *"more manageable (approach) for an average user"* [32].

To return to the relevancy of compressive fracture energy, such a material parameter allows to define a certain flexibility in the ductility of over-reinforced concrete under stress. In *Diana FEA* (a similar FEA software) compressive fracture energy G_c is possible to define by using ambient variables like temperature, concentration and maturity [33]. Additionally, under the *"Guidelines for Nonlinear Finite Element Analysis of Concrete Structures"* [34], it is recommended to make use of a model that is based on compressive fracture energy, [35, 36], and then using crushing band-width limitation (like [31]) to regularise the effect.

In the guidelines, [34], the compressive softening function is described by compressive fracture energy, G_c, which in turn is defined by the tensile fracture energy, G_f. A parabolic function illustrates the effect of the compressive fracture energy when introducing the ratio G_c/h, which allows for customisable ductility in the model, see Figure 9.

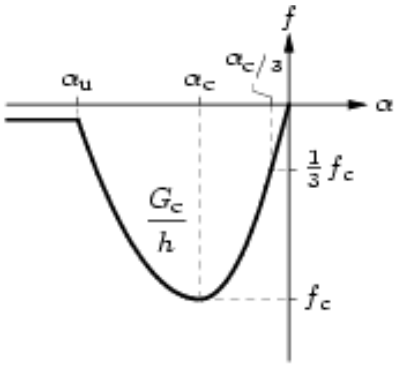

Fracture energy	$G_F = 73\, f_{cm}^{0.18}$
Compressive fracture energy,	$G_C = 250\, G_F$

Figure 9: Parabolic compression diagram (left) and definitions of Gf and Gc (right), [34].

2.8. Previous sensitivity analysis

As a pre-study ahead of this thesis, a very limited sensitivity study was conducted with a lower strength concrete type in Markeset's doctorate [3], namely the concrete dubbed ND25. In this short study, a wide range of inputs were tested to see the difference in response in order to achieve a brief expectation of what should be observed in the work this thesis presents. Since this previous work is not included here (due to plagiarism policy), the current chapter aims to briefly explain which expectations the authors have for the thesis, as well as what parts of the study should be limited – for various reasons. The information presented in this chapter is solely gathered in the mentioned pre-study and is not related to any new discoveries and realisations in regard to the work of this current thesis.

2.8.1. Expectations

The pre-study aimed to recreate the behaviour of a low-strength ND25 concrete was based on the same experimental data used for this thesis. A variety of results were observed, with some being considered close to irrelevant to observe due to their low impact on the simulations.

a. Abaqus FEA as a tool: Based on a limited literature study, Abaqus FEA is considered a precise tool for recreating and predicting material behaviour – but the program relies *heavily* on detailed and highly accurate and specialised inputs for the results to be considered valid. This high-accuracy expectation is carried over to the current work performed, while it is understood that a deep specialisation may not be feasible within the current time frame of the work.
b. The Dilation Angle: Altering the Dilation Angle parameter generally yielded the most variation in response in the analyses. The difference from one analysis with a high degree of Dilation, to another analysis with a low degree of Dilation, was observed as significant. It is expected to see a similar type of response based on the Dilation Angle of the higher strength concrete types. The pre-study discovered that an angle of 15 degrees yielded the results closest to those from the experiments.
c. fb0/fc0: The ratio of initial equibiaxial compressive yield stress to initial uniaxial compressive yield stress was also observed as a high-influence parameter. This parameter showed large differences in behaviour, and it was found that values lower than *1* was highly unrealistic for the various analyses. This expectation is also realised in the current work, as shown by the theory chapter regarding this parameter and what the value represents. It was also found that other studies of the parameter would tend to stick to the standard value of 1.16, with very limited deep-dive research on the parameter itself being available.
d. K_c: The ratio of the second stress invariants was found to create some odd behavioural changes when altered. While a general recommendation *not* to deviate from the standard value of 0.6667, it was found that a higher value proved beneficial for the pre-study work. Lower values would create strange responses that were considered unreliable and unrealistic, and thus should be avoided in this work. It was found that nearly all research regarding this parameter recommended or utilised the standard value.

e. The effect of going higher than the standard values: It was observed that increasing the values of *fb0/fc0* and K_c proved useful in more accurately replicating the experimental results. Meanwhile, lowering these two values below the standards would yield results that heavily deviated from the goal of the pre-study – as mentioned under points ***c.*** and ***d.*** It is expected that similar behaviour will be observed, and the authors enter the study with an expectation that combining these increased values may prove beneficial.

2.8.2. Limitations

While certain opportunities and expectations were made with the pre-study, it is also worth noting that certain limitations were observed as well. Some of the limitations identified in the pre-study has been expected to carry a similar amount of significancy in the current study and are listed below. These limitations serve as an important foot-note in the work presented here; some may be circumvented in further work with better equipment, and some may not be as easy to circumnavigate – if at all.

a. A greater amount of laboratory values was needed to increase the level of accuracy of the analyses. The authors had a limited range of base values to initiate the modelling, while the remaining values were figured out using the theory presented in this thesis – thus having to rely on theoretical approximations rather than fully accurate values.
b. Computing power: The authors of the paper was from an early stage forced to accept that being limited by computational resources was and is a major factor of the project work. The CDP simulations proved expensive in terms of computer work which in turn meant the various analyses took a significant amount of time. This time-constraint has been expected to also make a significant impact on the current work; Thus, highlighting the importance of finding a balance between mesh detail and simulation run-time.
c. Element amount: With an academic license of Abaqus FEA, there is a limitation to the number of finite elements allowed to include in the model. This varies based on the license, but in the authors' case the limit has periodically changed from 100.000 elements to 250.000 elements. While this sounds like a lot, the amount of elements in even small models rapidly approach these values when testing for mesh sensitivity. The practical limitation this introduces is the size of elements in the model: For a larger model, a more coarse mesh is not only necessary to consider for computational cost reduction but is unavoidable due to the license available to the authors.

2.9. A review of previous work on CDP

In order to gain an understanding of previous work on Concrete Damaged Plasticity for the purpose of comparison and discussion, a quick investigation of previous CDP work has been performed. The studies presented in this sub-chapter will, in one way or another, have presented work made on CDP either in Abaqus FEA directly, or in independent settings and/or other programs with similar models.

In *"The influence of shear connection strength and stiffness on the resistance of steel-concrete composite sandwich panels to out-of-plane forces"* by Philip Francis, [29], a study on the influence of shear connections and stiffness in regard to steel-concrete composite panels is conducted. Francis runs simulations in both Abaqus FEA and Ansys to investigate three design checks related to out-of-plane loads in said composite panels. In the doctorate, an original code script is developed to describe the stiffness reduction factor of the CDP model (Damage parameter), rather than using the given stiffness reduction parameter in CDP. The need to develop original code underlines the limitations of the "raw" CDP model parameters.

In the study *"Simplified Damage Plasticity Model for Concrete"* by Milad Hafezolghorani *et al.* [37], the CDP model is modified for simplified implementation of the stiffness reduction factor. Extended research in Hafezolghorani *et al.*'s study suggests that representing reinforced concrete structures with the CDP model is complicated, and the authors' decision to simplify the CDP model indicates various challenges related to accurately representing (reinforced) concrete in CDP.

In the research conducted by Michał Szczecina and Andrzej Winnicki – *"Calibration of the CDP model parameters in Abaqus"* [38] – the dilation angle and viscosity parameter are studied on two specimens: A concrete disc under uniaxial and biaxial compression, and a notched bar for uniaxial tension. This research concludes with a recommendation to use a dilation angle of 5 degrees and a viscosity parameter of 0.0001. This conclusion suggests a dilation angle far below the standard recommendation of 30-40 degrees, and the authors suggest that using a higher dilation angle would implement artificial increase of bearing capacity for confinement. This study again indicates the lack of consensus on a single, narrow range of parameter values – further reinforcing the indication that the CDP model requires specialised optimisation on a case-by-case basis.

"Study on concrete damaged plasticity model for simulating the hysteretic behavior of RC shear wall" by Q. Wang et al. [39] suggests that the damage parameter in CDP is inadequate for their problem scenario. Q. Wang et al. determine that utilising a concrete model from a different software (The *Concrete02 model* in *OpenSees*, a software framework owned and licensed by *The Regents of the University of California*) is necessary to properly define the CDP material model parameters.

Dragan M. Rakić et al. and their research in *"Concrete Damage Plasticity Material Model Parameters Identification"* [25] is a sensitivity study with similar research goals as this thesis. Experimental data from uniaxial tensile and compressive load-unload testing is used to determine material data, in order to define the concrete behaviour in CDP. Rakić et al. concludes that for uniaxial compressive and tensile analysis, the CDP material model is adequate when calibrated properly using experimental data for the various parameters. It

should be noted that the research also points out the lack of applicability of these uniaxial testing results to biaxial and triaxial experiments.

In *"Using the Abaqus CDP model in impact simulations"* by Alexis Fedoroff and Kim Calonius [40], Concrete Damaged Plasticity is used as a base for the development of an extension of the CDP model in order to simulate the effects of missile impacts on concrete. The study concludes that certain accuracy is achieved, however the model and the element removal algorithms are highly sensitive to the dilation angle value. Fedoroff and Calonius reinforce the theory that CDP is heavily dependent on the dilation angle parameter, and also reaffirm the fact that there is no single dilation angle value that is agreed upon for use of CDP.

3. Creating the Abaqus model based on the experimental data

This chapter intends to show what the models used for this research look like, including data from the laboratory experiments that has been the foundation for a large part of the modelling, [3]. The purpose of this thesis is to attempt recreation of various tests conducted by Professor Markeset [3], and includes a section of concrete cylinder compressive testing as well as a 4-point bending test of a reinforced concrete beam. These test specimens have been recreated in Abaqus/CAE, and consequently simulated with the relevant testing parameters.

3.1. Cylinder models

In general, the cylinders have similar geometric properties from the beginning. Two of the three cylinders presented in the laboratory results have the same dimensions, while the ND90-concrete cylinder was made somewhat more slender than the two weaker concrete types. In an attempt to save some time, the authors chose to model all three concrete types as a single geometrical model instead of differentiating between the two weaker concrete types and the ND90 Cylinder. Following guidance from the thesis supervisor, the primary assumption here was that the overall impact should not be too significant, but the discrepancy should regardless be given some attention when regarding the ND90-results later. The model size utilised for the analyses of the concrete cylinders was that of 145x295 (*DxL*), see Figure 10.

Concrete type	f_c (MPa)	D (mm)	L (mm)
ND25	22.2	145	295
ND55	45.3	145	295
ND90	70.0	100	285
LWA60	55.8	145	295

Figure 10: Concrete cylinder strength, diameter, and height/length as given in the doctorate. [3]

The cylinder required simple modelling as there were no reinforcing bars or adjective parts that needed to be considered. A 3D deformable, solid cylindrical structure was modelled and partitioned, as the partitions made it more efficient to assign loads and boundary conditions.

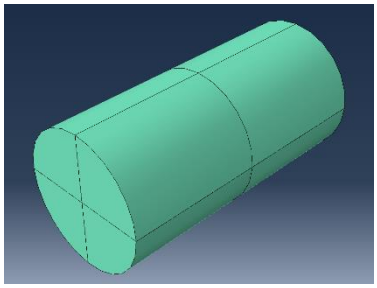

Figure 11: Partitioned cylinder model

The model was given material properties that matched those of the doctorate by Markeset [3], utilising the given elastic property values like the Young's modulus and Poisson's ratio and the stress-strain properties taken from the curves as shown in chapter 2.3, Figure 4**.** The remaining properties of the CDP model were initially set within their recommended standard values, while the compressive and tensile damage properties were set using the method as shown in chapter 2.6.9, using stress-strain data to convert values into inelastic strain parameters.

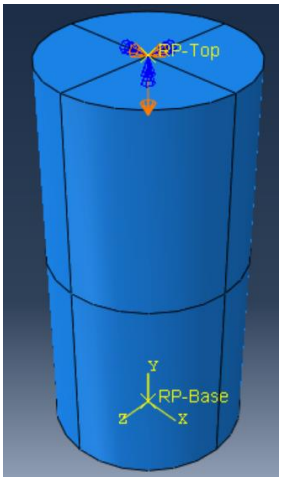

Figure 12: Cylinder with load conditions

The load was assigned at the top of the cylinder as a displacement over time. The bottom of the cylinder was fixed in every direction as it was not supposed to have any movement. Utilising reference points, the whole top and bottom surfaces were assigned as single units, essentially telling the model that any deformation in the Y-direction in the top was to be applied to the whole top surface. This ensured that the displacement applied would behave like a concrete compressive loading test would.

Following application of these properties, the loading cycle was defined. Applying a total loading time and time step size in Abaqus/Explicit entailed a few more considerations than what would be required in Abaqus/Standard (implicit). The loading was applied over multiple different time periods in the analyses, but largely with a time period of 1-5. Time steps were given a minimum and maximum parameter in order to achieve a balance of data amount and computing time.

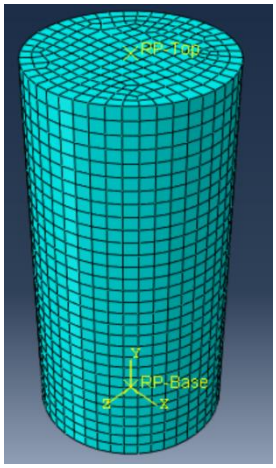

Figure 13: Cylinder mesh

The model elements were given a global element size of 15 for the ND25 and ND55 Cylinders and a size of 10 for the ND90 tests, allowing for relatively decent element size and acceptable accuracy in the simulations. A few tests of element size 3 was conducted (yielding approximately 220.000 elements, just below the maximum allowed under the academical license of Abaqus), and this testing proved that there was little difference between an element size of 10 and 3. Going below element size 3 was not possible as this would exceed the license limit. The mesh type is *C3D8(R)*, a mesh type commonly used in a large range of Abaqus simulations. This mesh included hourglass controls, and the *R* in the element name refers to *reduced integration*. The parathesis is there to imply that both reduced and full integration methods have been used in the analyses, yielding improvements in certain areas – more on that in chapter 4: Findings.

3.2. Beam models

The beam was a more complicated assembly than the cylinder as it required more parts. The main component was the concrete beam and its steel rebar, with various rebar- and stirrup types included in each model.

The Abaqus beam was modelled after the specifications given in the doctorate, with a range of important details to consider, see Figure 14 [3] showcasing one half (left) of the beam; the left and right side of the middle was identical. Take special note of the difference in cross-section A-A and cross-section B-B: The bottom middle section of the beam was unreinforced, something that was important to catch in the finite element model applied in Abaqus. This section could be left unreinforced due to the nature of the loading setup.

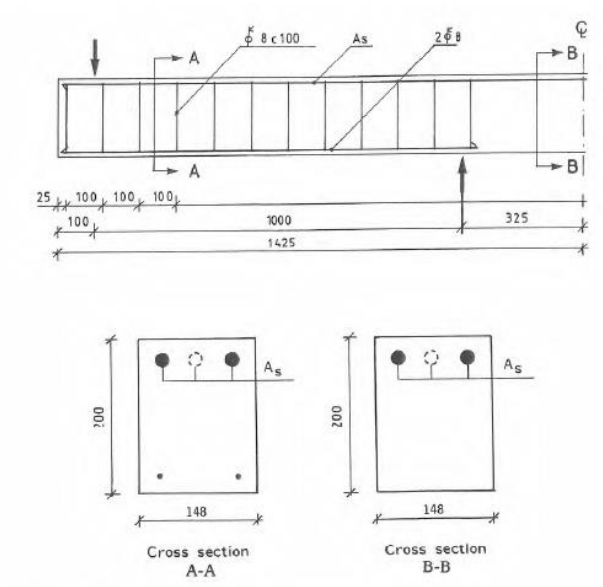

Figure 14: Lab beam specifications, from Markeset [3].

See Figure 15 [3] for the specific properties related to the concrete and reinforcement of the beams.

Beam identity [1]	Cube strength (MPa) [2]	Number of beams	Tensile reinforcement		
			A_s (mm)	f_y (MPa)	Type
ND25-u	24.5	2	2ϕ12= 226	408	K400TS
ND55-u	54.8	2	3ϕ12= 339	408	K400TS
ND90-u	84.6	2	2ϕ16= 402	555	K500TS
ND25-o	23.4	2	3ϕ20= 943	469	K400TS
ND55-o	53.2	2	2ϕ32=1609	587	K500TS
ND90-o	85.4	2	2ϕ32=1609	587	K500TS
LWA60-o	57.2	2	3ϕ20= 942	574	K500TS

[1] Extension -u and -o means under- and over-reinforced, respectively.
[2] Mean compressive strength on six 100x100 mm cubes from two batches at 14 days.

Figure 15: Material data, [3]

For the loading setup, an inverted 4-point bending test, loading the beam from the bottom, and upwards using two hydraulic jacks, was conducted in the laboratory experiments, see Figure 16 [3]. This setup was also translated into the Abaqus model in order to observe the effect this would have.

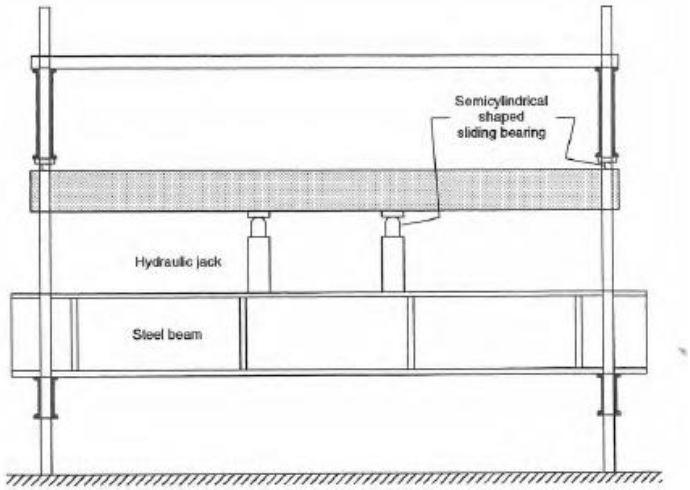

Figure 16: Sketch of the experimental beam loading setup, [3].

The Abaqus model followed the specifications given by Markeset's doctorate, [3]. Dimensions and rebar sizes utilised followed the *-o extension* as noted in Figure 15, recreating the various beam types as accurately as possible for the three concrete strengths.

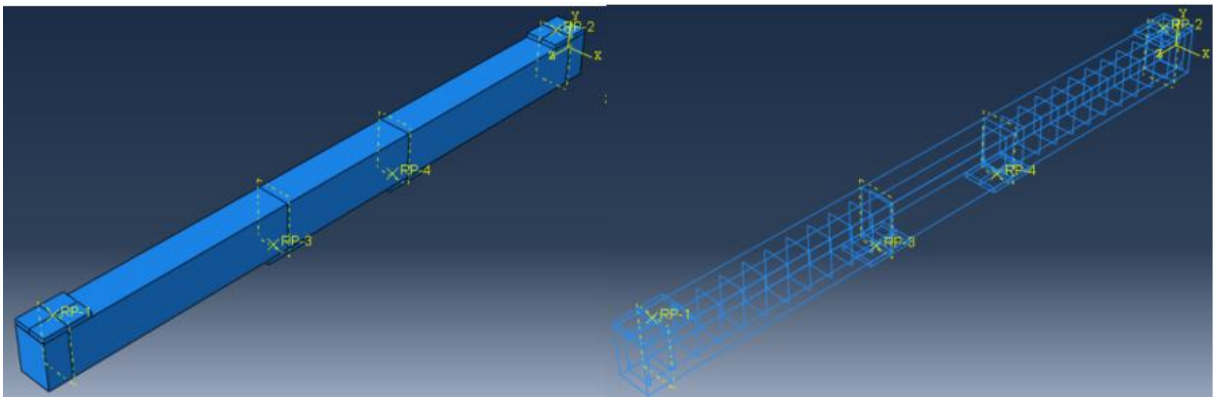

Figure 17: Beam model in Abaqus, solid concrete (left) and reinforcement setup (right) with given reference points

For mesh sizes, the concrete beam was given a global mesh size of 50, while the reinforcement bars were set with a mesh size of 30. While the mesh size ideally would have been made smaller, a combination of the limitations in computing power (in regard to analysis time) – and an upper limit of how many elements the authors were allowed to run with using the academic package of Abaqus FEA – restricted the ability to use much finer meshes than what was used for this research. The mesh combination of 50 and 30 for concrete and reinforcement, respectively, allowed for multiple analyses to be conducted in an attempt to optimise settings, without each analysis taking far too long to be considered reasonable given the time constraints tied with this thesis.

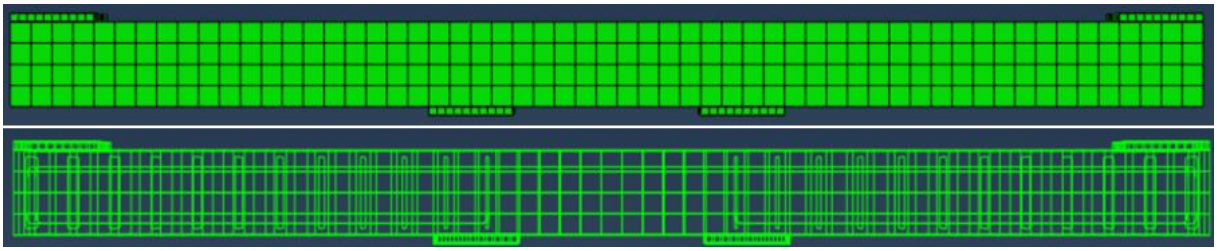

Figure 18: Beam mesh sizes

The supports and loading plates were initially modelled as cylindrical shapes, with the curved edge pressing towards the beam, to simulate as accurate of a point load as possible. Some issues with the analyses that were attempted using this shape led to a redesign of these nodes, creating flat loading/support conditions instead.

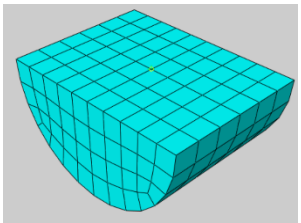

Figure 19: Initial shape of load/support

Figure 20 illustrates how the flat shaped load/support surfaces moved in relation to each other. The left/right edge were static, while the two bottom supports bended the beam upwards.

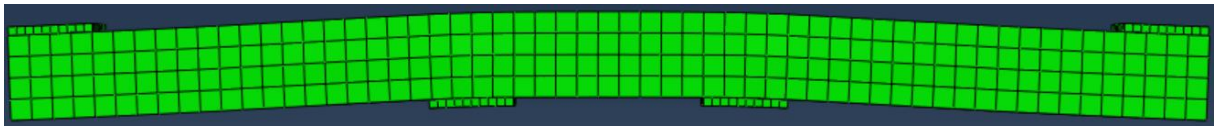

Figure 20: Beam in deformed position

A deformation of 50mm was set for each of the loading plates, directed upwards into the overlaying beam. This forced the beam to bend in a similar fashion to that of the laboratory experiments. An important difference to note between this loading scenario and that of the experiments, is that the deformation was applied as a single load step. Ideally, multiple load steps with paused intervals between would have been utilised similar to those conducted in the doctorate of Professor Markeset [3], but this proved exponentially more expensive computationally. Thus, a single load step for the entire deformation was applied.

To record the results, a time-history output was requested prior to analysis. The reference points given in Figure 17 were given time-history requests of displacement and load response in order to then record the responding curves of the beam models under deformation. The modelling results were then intended for comparison against the stress-strain curvature given in Markeset's doctorate, see Figure 21 [3].

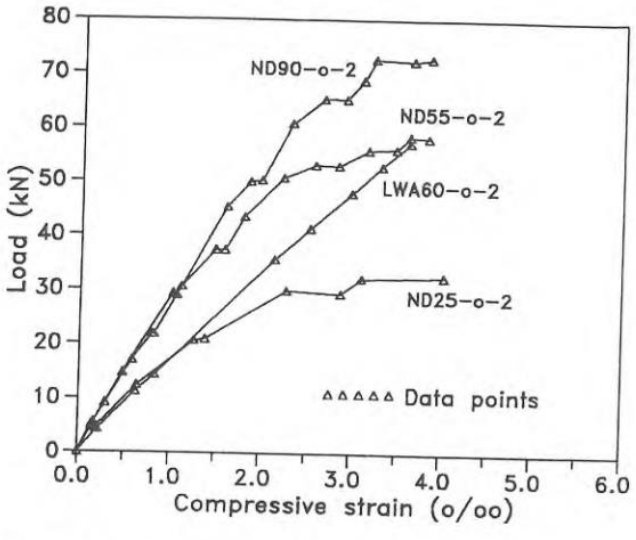

Figure 21: Average concrete compressive strain for over-reinforced RC beam. [3]

4. Findings

4.1. Cylinder test plastic strain conversion

The output obtained from Abaqus was given in Stress-plastic strain, therefore the stress-strain graph in the doctorate was converted into stress-plastic strain.

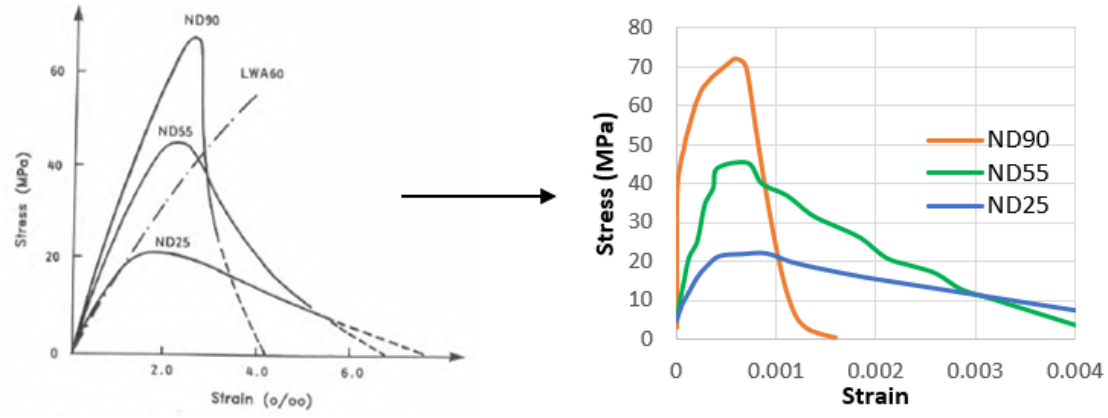

Figure 22: Stress-Strain to Stress-Plastic Strain conversion. To the left, the plots from the doctorate [3]. To the right, the converted plots, using the theory for plastic strain conversion from chapter 2.6.9, Eq. 29.

The results shown in this chapter was achieved by adjusting the different parameters to figure out how they altered the curves. The objective was to find which parameters gave the best comparison to the physical tests.

In the graphs below the black curve will always be the stress-plastic strain curve calculated from the physical tests and the red curve obtained from Abaqus with “standard” values. There will be other colours displayed as well, these will represent the different parameters tested.

For some of the parameters the results were not reasonable after the yield strength was met as they got a linear softening curve as a result of the stress output jumping to zero or almost zero and at the same time the stress jumped to almost maximum or almost maximum. No particular reason was found as to why this was happening as no literature addressing this issue was found during the research.

There was reason to believe that with higher strength concrete Abaqus had difficulties registering the drop happening in the softening part of the curve. This was mainly a problem for the ND90 concrete and also for some parameters in the ND55 concrete, there was also a few instances where this became a problem with the ND25. However, this only occurred when the properties were altered out of “regular” proportions.

As the problem was consistent through the ND90 model it was not reasonable to evaluate the output Abaqus gave after the material yielded. The authors had the same problem with the ND55 concrete but were able to fix the problem by removing the reduced integration option for the mesh-type. Where this problem occurred, it will be mentioned in the respective segment where it is presented.

In the end of the parameter test of each concrete type, a combination of parameters was implemented to produce the best available stress-plastic strain cure compared to the laboratory tests.

4.2. Investigated parameter values

To gain an understanding of how each core parameter of CDP impacted the simulations, a set of values was decided upon to be used on each of the concrete qualities. The parameter values utilised in the analyses are presented below, and these values are generally in line with what previous researchers have attempted when doing sensitivity analyses of Abaqus and/or CDP.

	ND25/55/90	**Standard parameter value**
Dilation Angle (degrees)	10 *(Except for ND55)* 15 25 45 55	30-40
Eccentricity	0 0.2 1	0.1
Fb0/Fc0	1 1.3 1.6	1.16
Kc	0.5 0.6 0.7 0.8 0.9 1	0.6667
Viscosity	0.0001 0.001	0

Table 2: CDP Parameter test values

**Note that a dilation angle of 10 degrees is excluded from the ND55 cylinder tests. More on that in chapter 4.4 ND55.*

4.3. ND25 Cylinder (*"C25"*)

4.3.1. Mesh sensitivity analysis

An initial investigation into the influence of the element size was conducted to determine the effect of the mesh. Certain differences were observed in the later parts of the analysis, with an element size of 10 leading to issues at the very end of the simulation. An element size of 15 was found to be adequate for the testing, yielding decent enough ductility and overall stress-strain development.

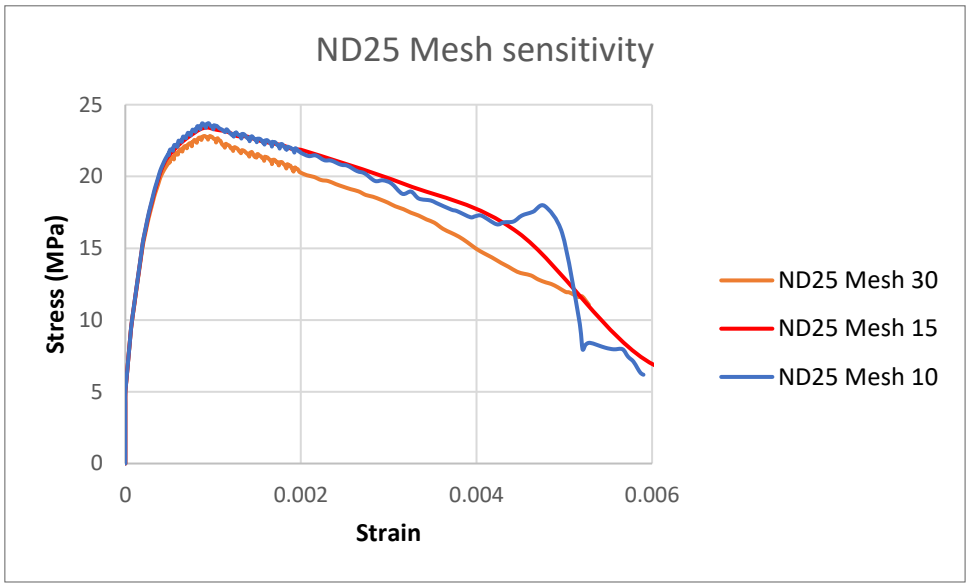

Figure 23: ND25 Mesh analysis

4.3.2. C25 Standard parameter values

The graphs had similar elastic regions but differed from peak compressive stress and continue down the softening curve. The ND25 Physical test curve indicate the desired result for the analyses that has been run, while the red ND25 Standard curve exhibits how the CDP model struggled to predict the post-yielding of the concrete using standard parameter values.

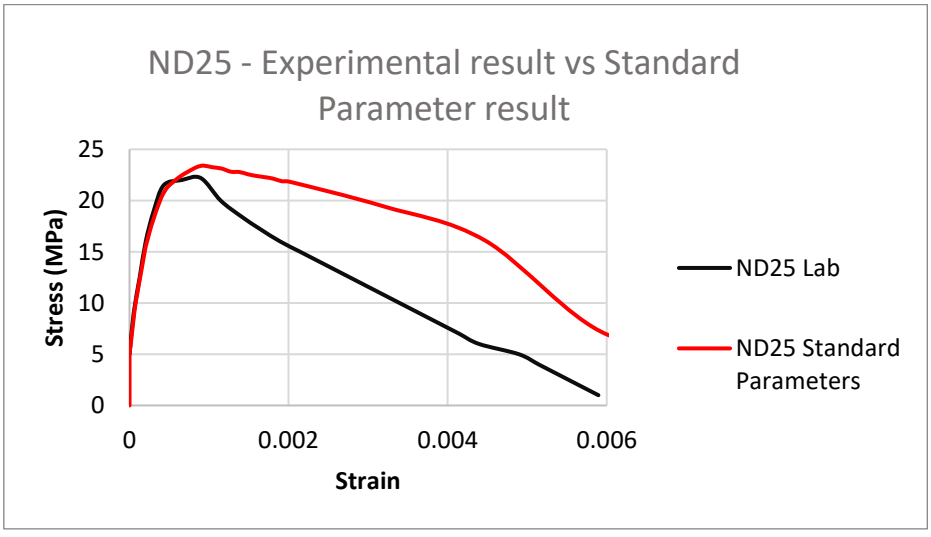

Figure 24: ND25 Baseline test

4.3.3. C25 Dilation angles

From theory it is recommended that the dilation angle is between 30-40 degrees, while lower values for the dilation angle gives material properties that are more brittle [26]. Angles in the rage of 10-55 degrees was tested to find the most accurate dilation angle compared to the experimental lab results.

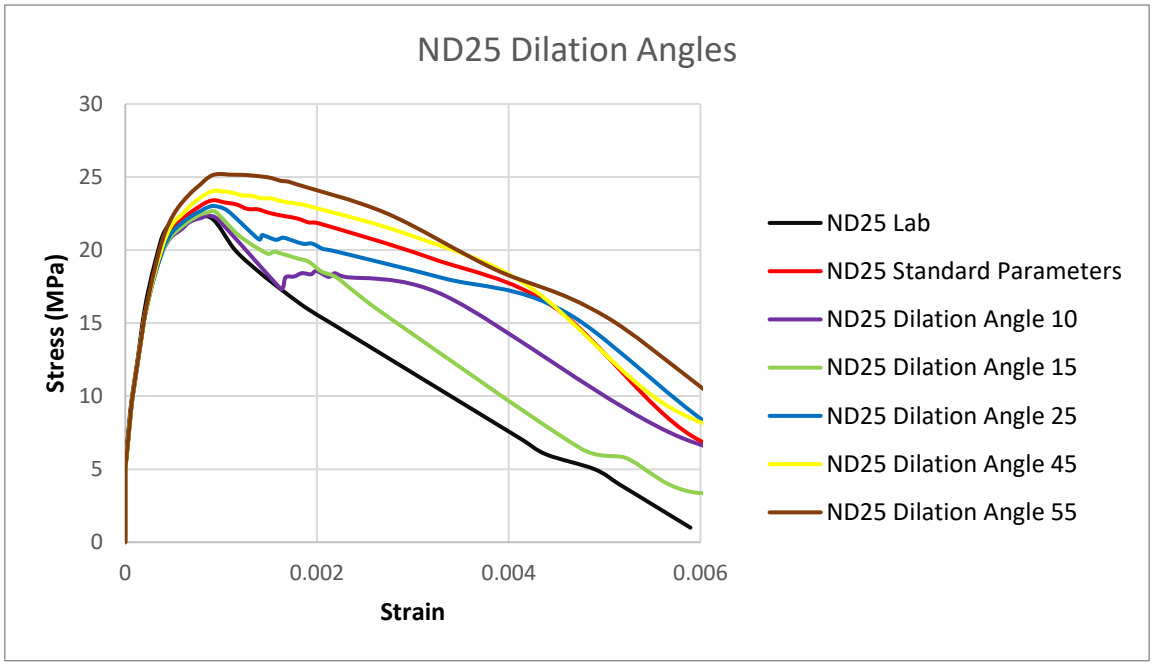

Figure 25: ND25 Dilation Angle

With decreasing angles of dilation, the stress-strain curvature's accuracy to the experimental results increased. Post-yielding behaviour appeared to be mostly similar, while 10 degrees of dilation produced an inconsistency with the softening.

A dilation angle of 15 seemed to be the most accurate compared to the laboratory test conducted by Markeset [3], but for the first part of the softening a dilation angle of 10 seemed to be a better match. However, as mentioned earlier in this chapter some inconsistencies happened when the material data was altered too much as Abaqus didn't give reasonable results. This appeared to be the case for dilation angle 10 as the stress suddenly increased in the softening part of the curve.

Regardless of the problems that occurred with a dilation angle of 10, the trend here was that with lower dilation angles the more desirable the results appeared.

4.3.4. C25 Eccentricity

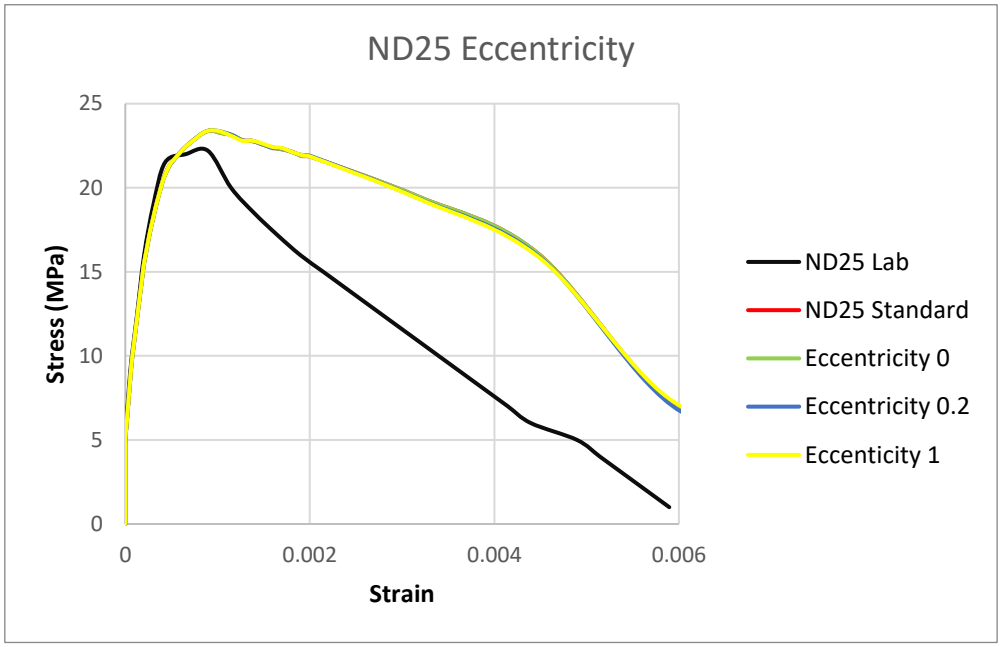

Figure 26: ND25 Eccentricity

There was no significant change in the result when we considered different values for eccentricity, see Figure 26. On its own, the eccentricity of concrete class ND25 had no visible impact on the resulting curves.

4.3.5. C25 Fb0/Fc0

The range of values tested here was from 1 to 1.6, lower values would not be reasonable as mentioned in chapter 2.6.6, and higher than 1.6 would indicate unreasonable increase in strength.

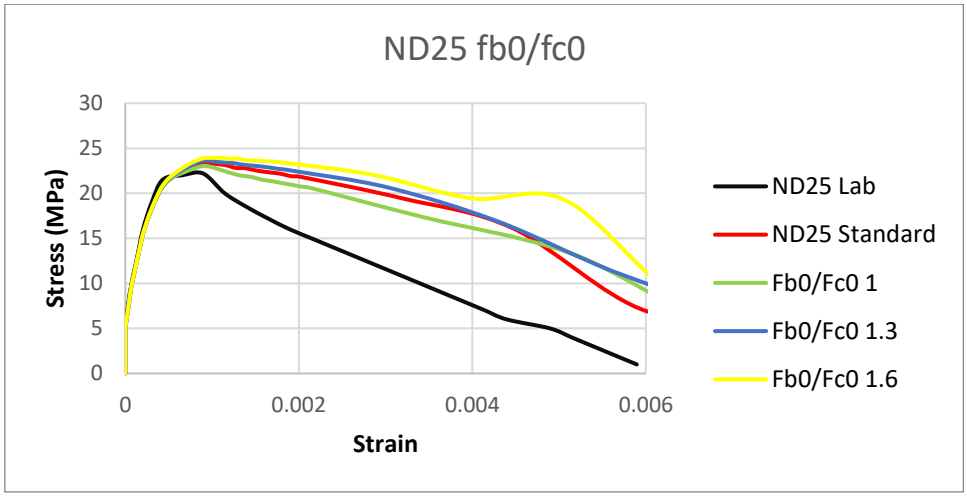

Figure 27: ND25 Fb0/Fc0

The softening curve trends toward the experimental result when reducing the ratio toward 1. This may indicate that the standard value of 1.16 for this concrete quality was too ductile to achieve similar results.

4.3.6. C25 Kc

The Kc parameter was tested between the limit values of 0.5 and 1, as mentioned in chapter 2.6.7.

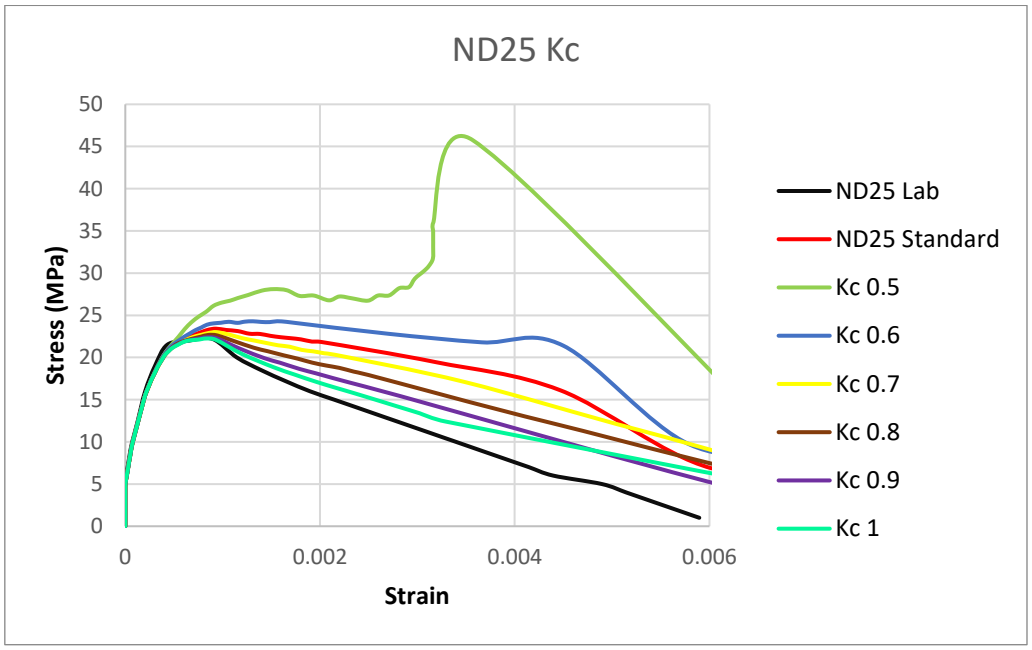

Figure 28: ND25 Kc

Kc 0.5 yielded an anomaly in regard to stress-strain curvature. As such, this value is considered completely irrelevant to consider. This was also disregarded as the analysis needed double the amount of displacement to get to the yielding point, indicating that the result should not be regarded as logical.

The other parameter tests matched every part of the curve obtained in the laboratory test as they only differed in the softening curve, where higher values seemed to be the best alternative for this concrete type.

4.3.7. C25 Viscosity parameter

The Viscosity parameter is usually used to resolve convergence that may occur when running the analysis. No such problems were encountered, but the parameters were still analysed to see if they had any impact on the results. Unsurprisingly, no changes to the curvature could be observed with different viscosity values.

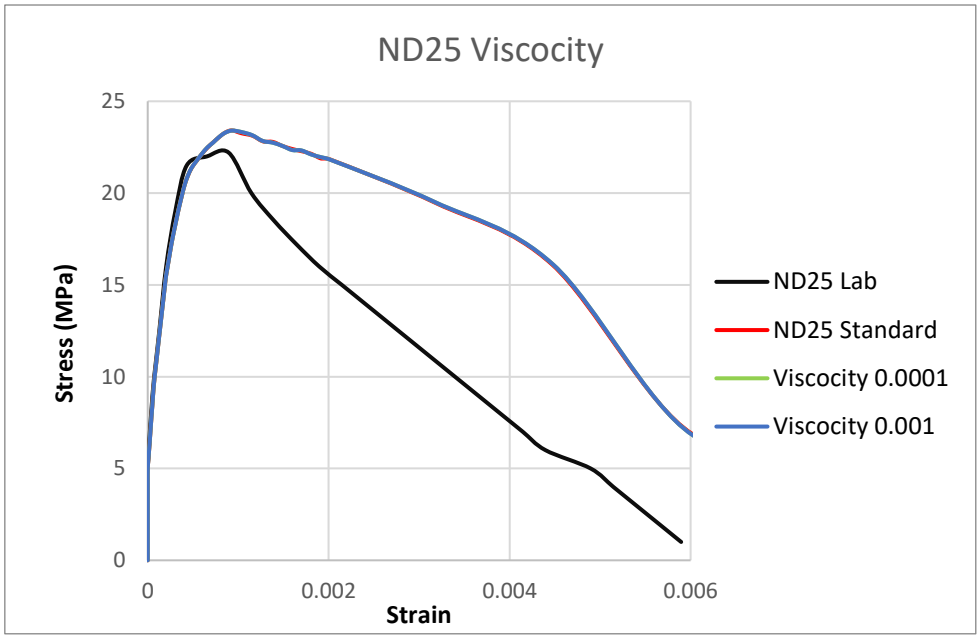

Figure 29: ND25 Viscosity parameter

4.3.8. C25 Optimal parameter combinations

To achieve the best possible result, a combination of parameters was needed to calibrate the stress-strain curve to the experimental result. In Figure 30, a couple of these optimisations can be observed to match the ND25 scenario well.

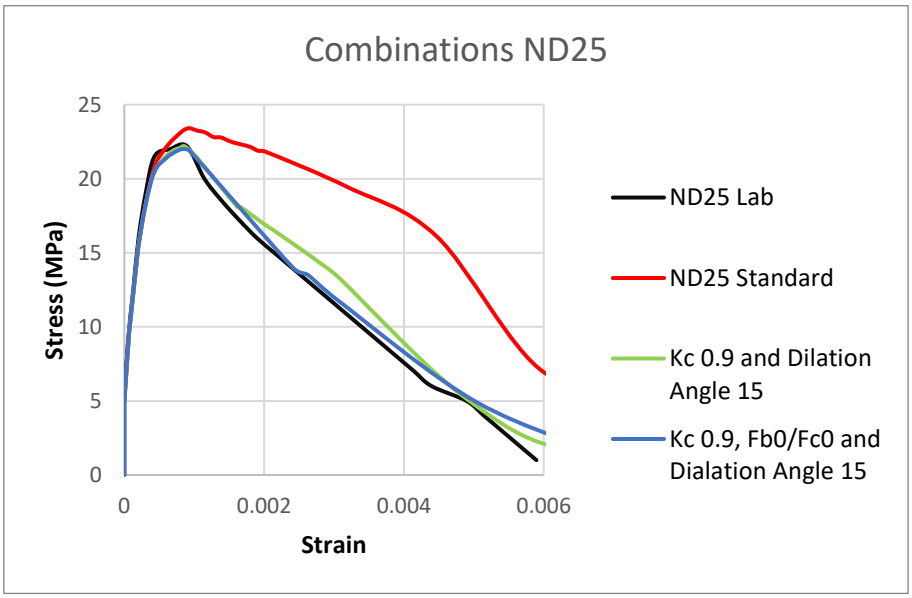

Figure 30: ND25 Parameter Optimisation

By observing the results from the different parameter tests individually it was mainly Kc, Dilation angle and Fb0/Fc0 that made a difference for the stress-plastic strain curves. First Kc 0.9 and Dilation Angle 15 was tested together as they showed promising results in their individual simulations. A Kc-value 1 could also be used, but as this is the maximum value for Kc there was a worry that it could result in unreadable or false curves in the softening part.

The first combination gave results like the laboratory test. However, the softening curve was still slightly off. The Fb0/Fc0 parameter at a ratio of 1 was enabled as it was a parameter that could alter the softening curve in the right direction.

The results with Kc 0.9 Fb0/Fc0 and Dilation Angle 15 is promising as the curve is almost identical to the laboratory test. It could have been tinkered with a bit more, but the result is sufficient to conclude what parameters should be for this concrete.

4.4. ND55 Cylinder (*"C55"*)

4.4.1. C55 Standard parameter values

With standard values given by Abaqus, the main issue was also the softening curve for ND55. As mentioned earlier in this chapter there were some issues with this concrete type regarding the softening curve. However, the problem was mainly fixed by using full integration.

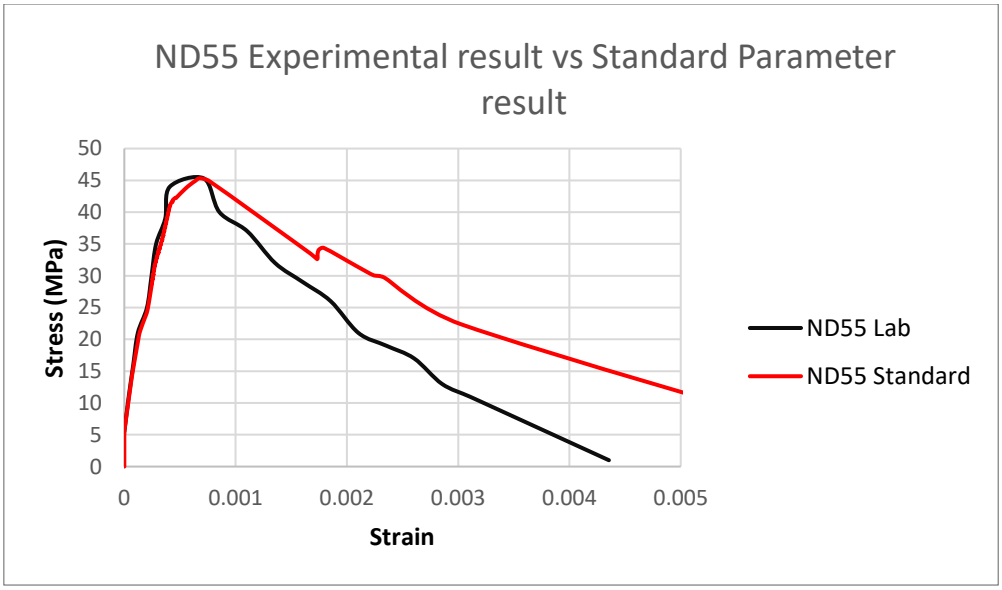

Figure 31: ND55 Baseline test

There is a small point in the softening curve for the standard parameters that stand out with a small increase in stress mid-softening. No way to resolve this issue was found as altering with the parameters and different mesh types and displacement durations would result in faulty analysis in the same manner as is explained earlier.

4.4.2. C55 Dilation angles

Same Dilation angles was tested for ND55 as for ND25, as the theory is still the same where values outside these parameters would not be realistic. One value was however skipped for ND55 as a Dilation angle of 10 would not be necessary to test as a Dilation angle of 15 didn't read realistic values.

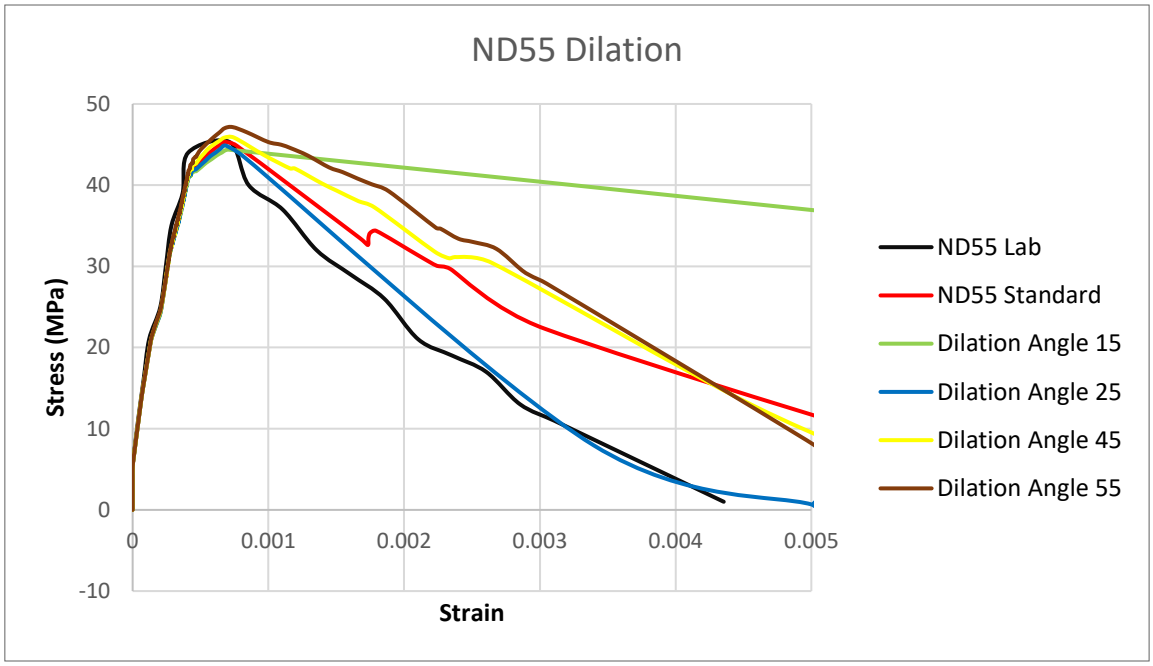

Figure 32: ND55 Dilation Angle

In Figure 32, the curve for Dilation Angle 15 shows the problem that have been discussed where the softening curve became a linear line that had no points between max strain and minimum stress. Therefore, this was not an option when combining parameters later.

When we consider the other values tested, they gradually got closer to the laboratory test as they got lower. Dilation angle 25 showed promising results as the curve was almost identical to what is the goal. This entails that the material was more brittle than the recommended values indicated.

4.4.3. C55 Eccentricity

Eccentricity was not expected to alter the results of ND55, but three alternatives' values from 0-1 were still tested to cover the possible outcomes.

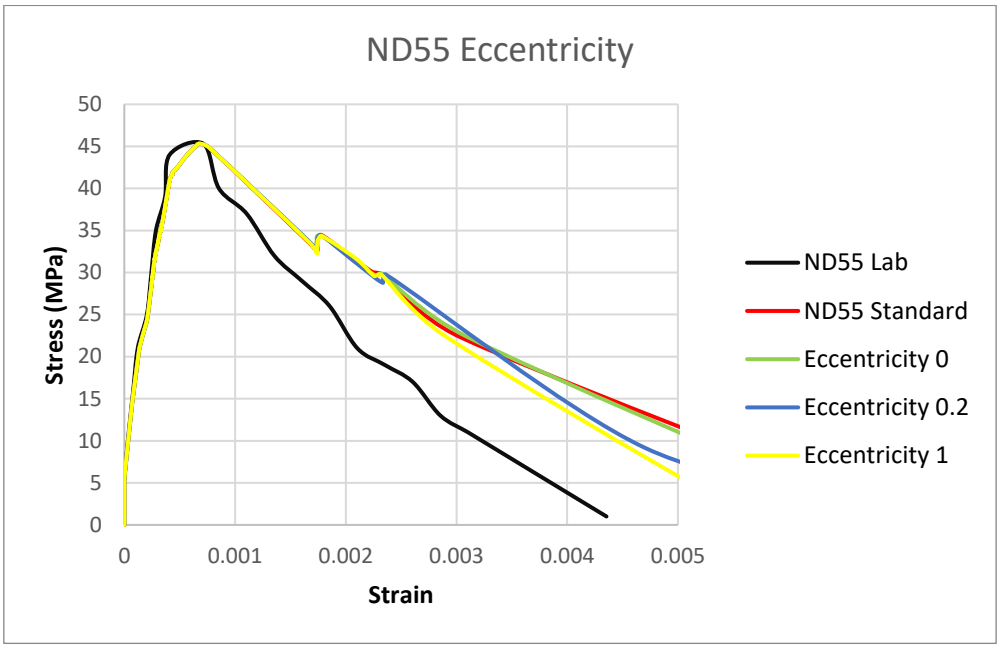

Figure 33: ND55 Eccentricity

4.4.4. C55 Fb0/Fc0

Parameters were tested similarly to the ND25 cylinders. They gave the same response until the softening curve and continued a way down the softening curve until there was a sudden jump in stress again. A ratio of 1 seemed to be the most agreeable for a while, but this ratio also experienced an inconsistency in the post-yielding phase.

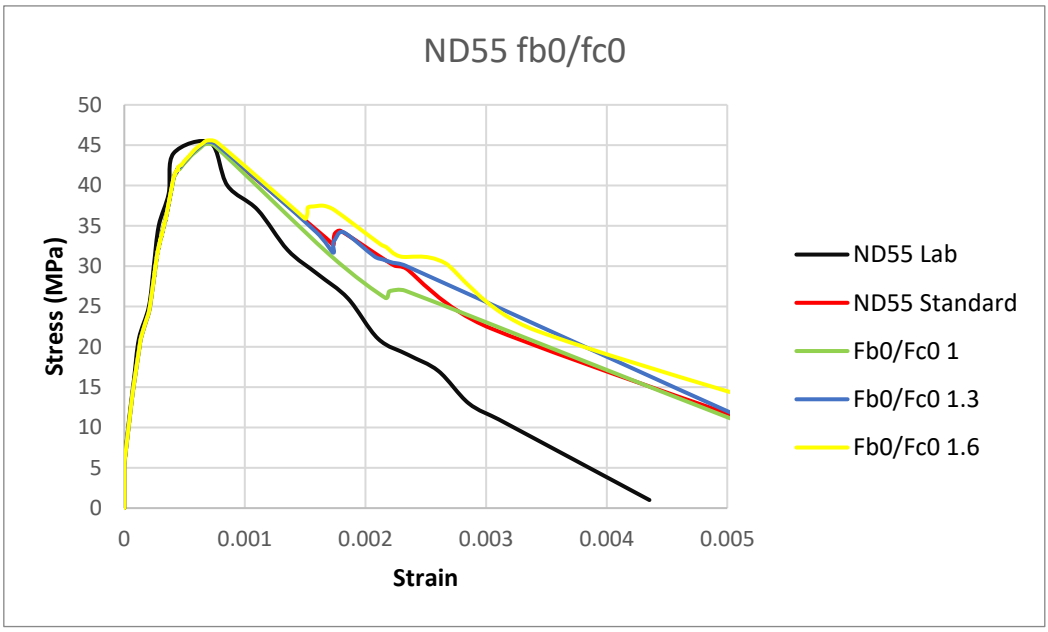

Figure 34: ND55 Fb0/Fc0

4.4.5. C55 Kc

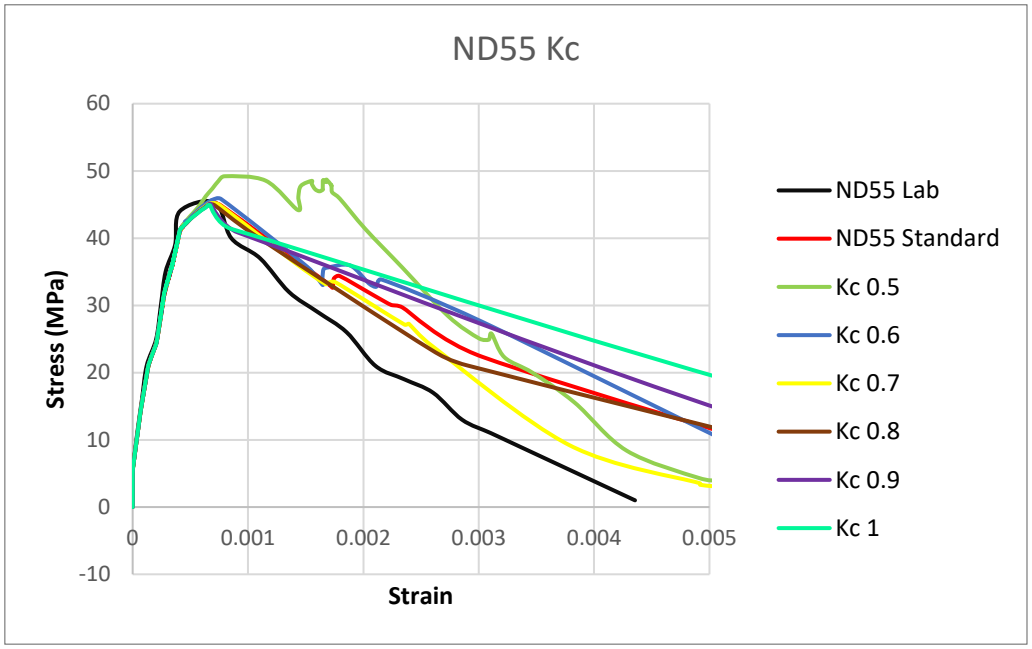

Figure 35: ND55 Kc

Kc 0.5 had higher ultimate stress than the rest of the analysis and was the furthest away from the identical curve. Kc 1 resulted in the linear post-yield behaviour as discussed at the beginning of the chapter – this was also the case for Kc 0.9.

Kc 0.6, 0.7 and 0.8 were all close to the curve with standard parameters, but Kc 0.7 was the one that showed the most promising result as it had a similar softening curve as the laboratory tests.

4.4.6. C55 Viscosity parameter

No problems with convergence were observed with ND55 either, therefore viscosity should not alter the curves any considered amount. Both viscosity values of 0.0001 and 0.001 did not alter the curves from the standard parameters.

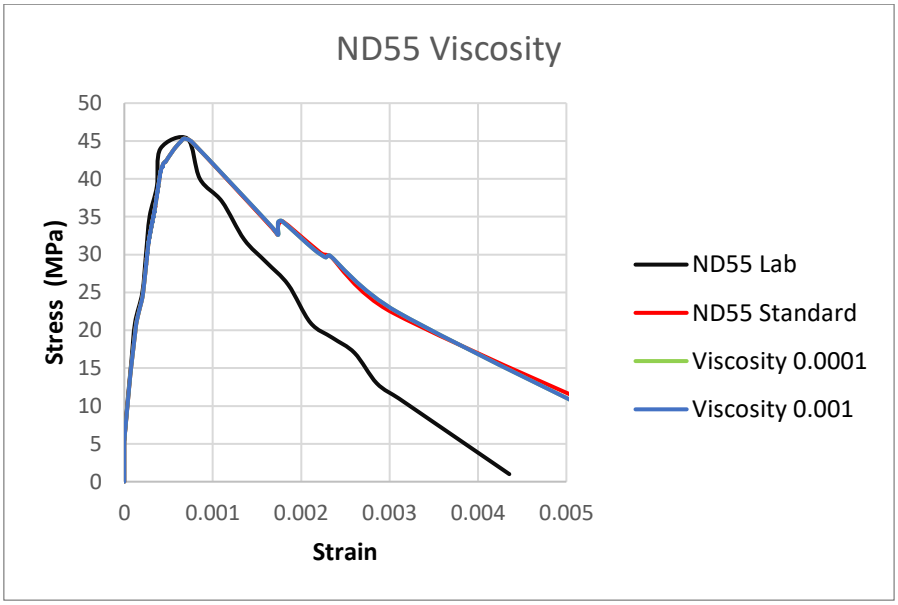

Figure 36: ND55 Viscosity parameter

4.4.7. C55 Optimal parameter combinations

The parameters that showed the most promising results were the same as for ND25, where Kc, Dilation Angle and Fb0/Fc0 were the ones that made a difference.

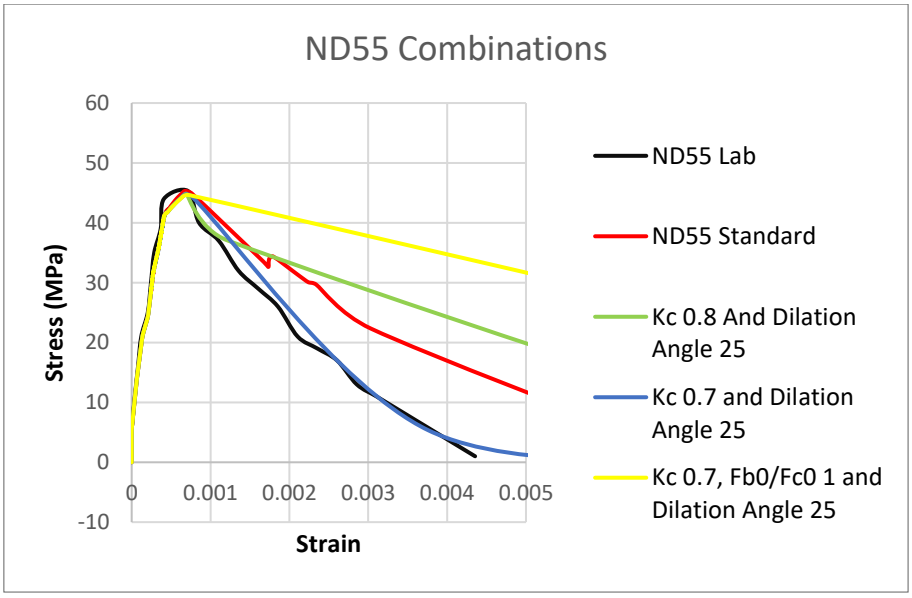

Figure 37: ND55 Parameter Optimisation

Three different opportunities were tested as they could give the best resemblance considering the laboratory test. The first test with Kc 0.8 and Dilation Angle 25 did not give a reasonable output as the same problem was encountered with a linear jump. This also showed how fragile the analysis for ND55 was as a combination of two parameters that worked fine by their own resulted in faulty results.

As Kc 0.8 resulted in issues, Kc 0.7 was tested as it was closer to the recommended values given by Abaqus and literature. This combined with Dilation angle 25 resulted in a near perfect resemblance of the laboratory test.

An additional test was done where Fb0/Fc0 ratio of 1 were added as for ND25, but this resulted in the same issue as the first test where the graph wasn't giving a usable result.

4.5. ND90 Cylinder (*"C90"*)

4.5.1. C90 Standard parameter values

Attempting to recreate the ND90 results proved to be more of a challenge than with the previous concrete qualities. The fixes that worked for ND25 and ND55, like dropping the reduced integration, did not translate to the ND90 simulations. A continued struggle to recreate the steep post-peak behaviour of the brittle concrete is the main take-away from the attempts to recreate this experiment for this concrete.

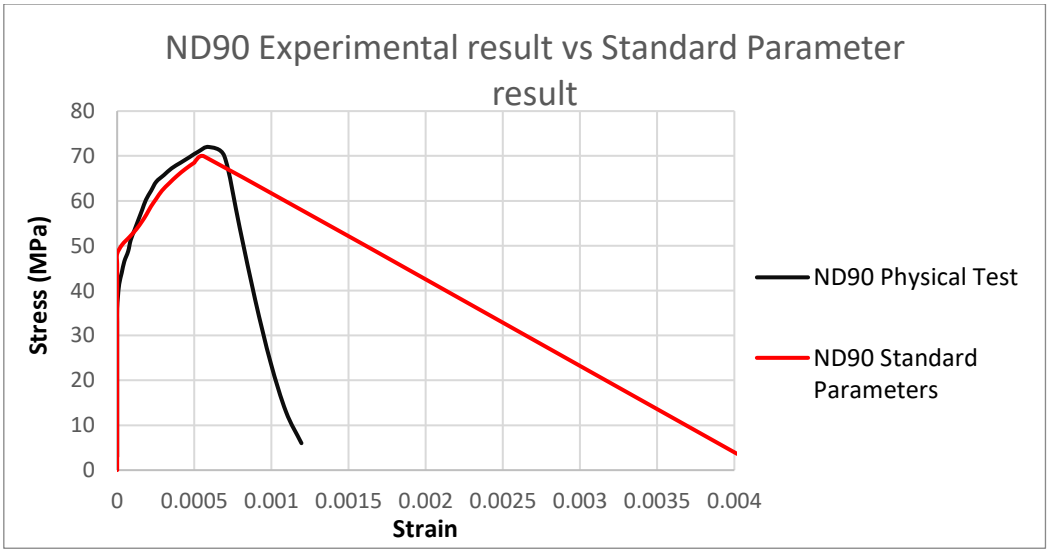

Figure 38: ND90 Baseline test

The Stress-Strain curvature can be observed as crudely similar to the physical lab results in the starting phases of its simulation, but as ultimate yield stress is reached, the software failed to record the softening behaviour using just standard parameter values. Observed in Figure 38, the linear behaviour was a reoccurring problem in the entire ND90 analysis.

4.5.2. C90 Dilation angles

The dilation angle's effect on the ND90 concrete appeared to be just as impactful as with the other concrete types – however, these changes did not yield any desirable post-yield behaviour similar to the laboratory testing. The major impact of the dilation angle appeared to relate to the rate of decline on the stress-strain relations, however. A little unexpectedly, the analyses running an angle of dilation of 10, 15 and 55 degrees appeared to yield the most relevant results.

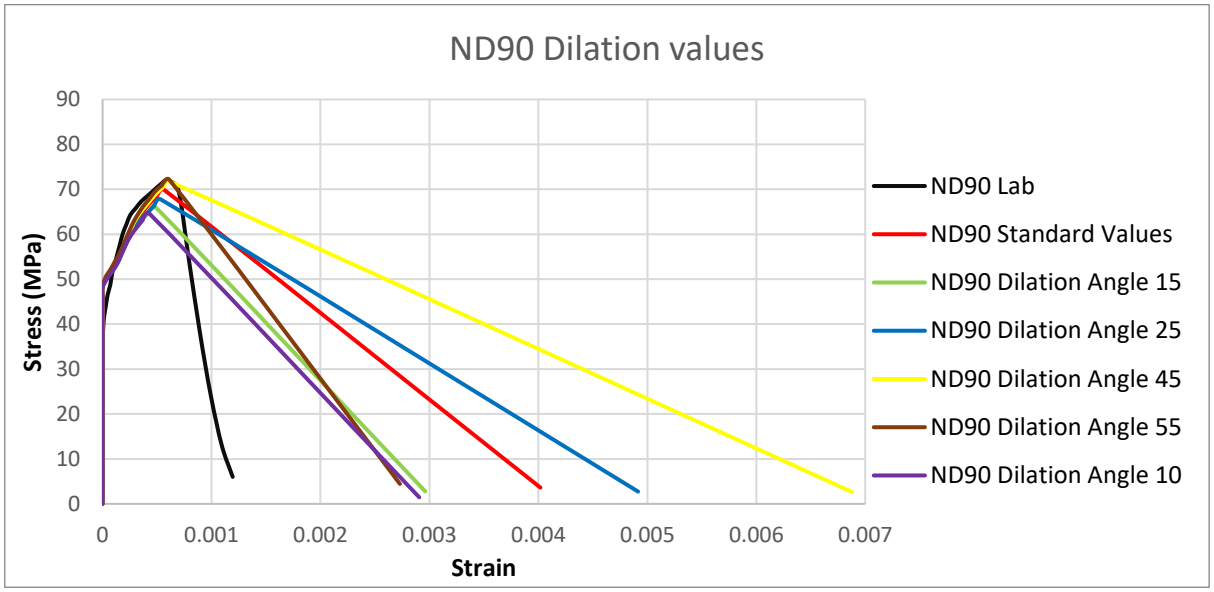

Figure 39: ND90 Dilation angles

The main issue remained with the ND90 concrete during the dilation angle tests; No desirable post-yield behaviour was shown, with a linear decline indicating that the simulation was unable to accurately plot the sudden destruction of the strong, but brittle concrete.

4.5.3. C90 Eccentricity

The effect of the eccentricity value appeared negligible, see Figure 40. The standard eccentricity of 0.1 yielded the exact same results as with an eccentricity of 0 – this was due to the eccentricity approaching 0 yielding a non-hyperbolic function, and thus the function became invalid for this model.

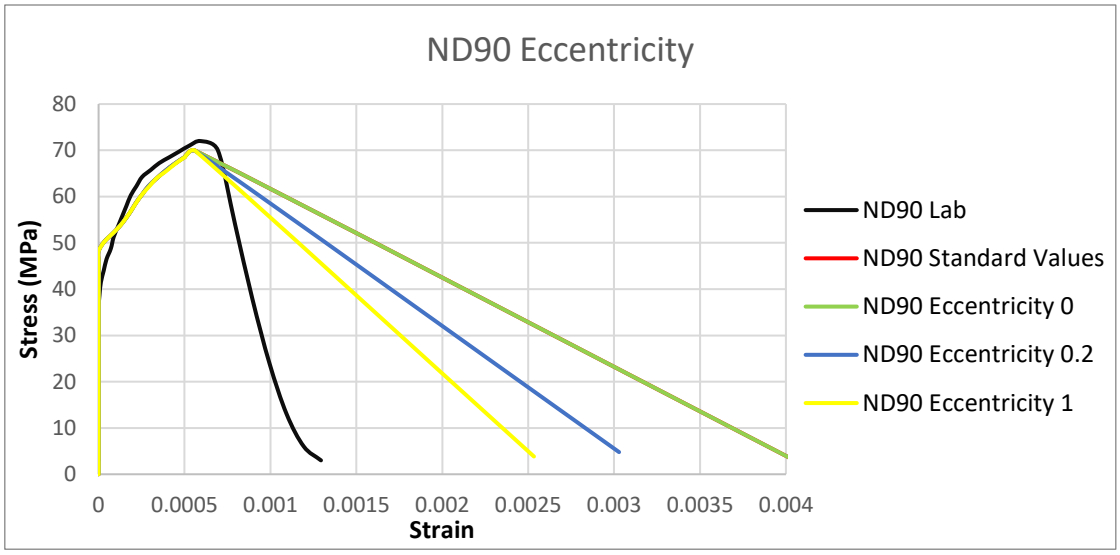

Figure 40: ND90 Eccentricity

Changing the eccentricity yielded, in general, results as expected with only very small changes to the post-yield phase. The issue with the linear stress-strain jump persisted.

4.5.4. C90 Fb0/Fc0

Regarding the ratio fb0/fc0, as discussed earlier going below a value of 1 was considered physically invalid. Testing values ranging from 1 to 1.6, including the standard 1.16, yielded a result that hints towards better post-yield behaviour – however, a discrepancy is still highly present. A ratio of 1.3 yielded the closest stress-strain relationship, with a ratio of 1.6 cutting a close second.

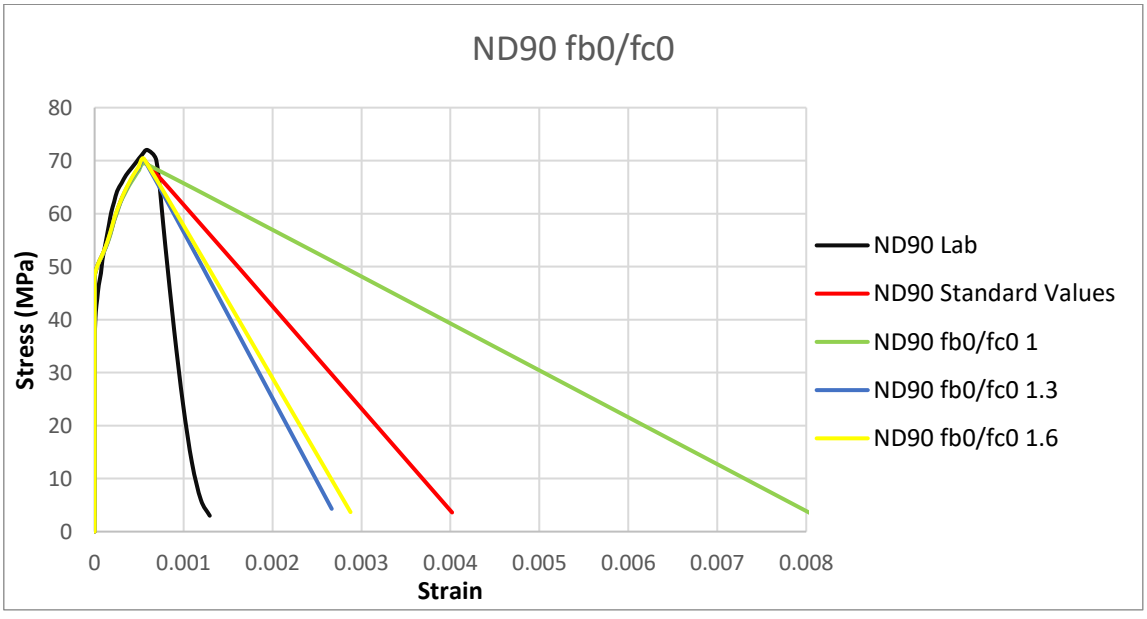

Figure 41: ND90 Fb0/Fc0

A certain promise was observed with the alteration of the fb0/fc0 ratio, but there was not a satisfying result with the ratio changes alone.

4.5.5. C90 Kc

The values for Kc were tested as previously with the lower standard concrete. It was here the first promising results were observed: Kc equal to 0.9 appeared to yield a very similar post-yield stress-strain decline to the lab test, with the rates of decline being near identical. The analysis still failed to model the failure as anything more than a linear relationship, however.

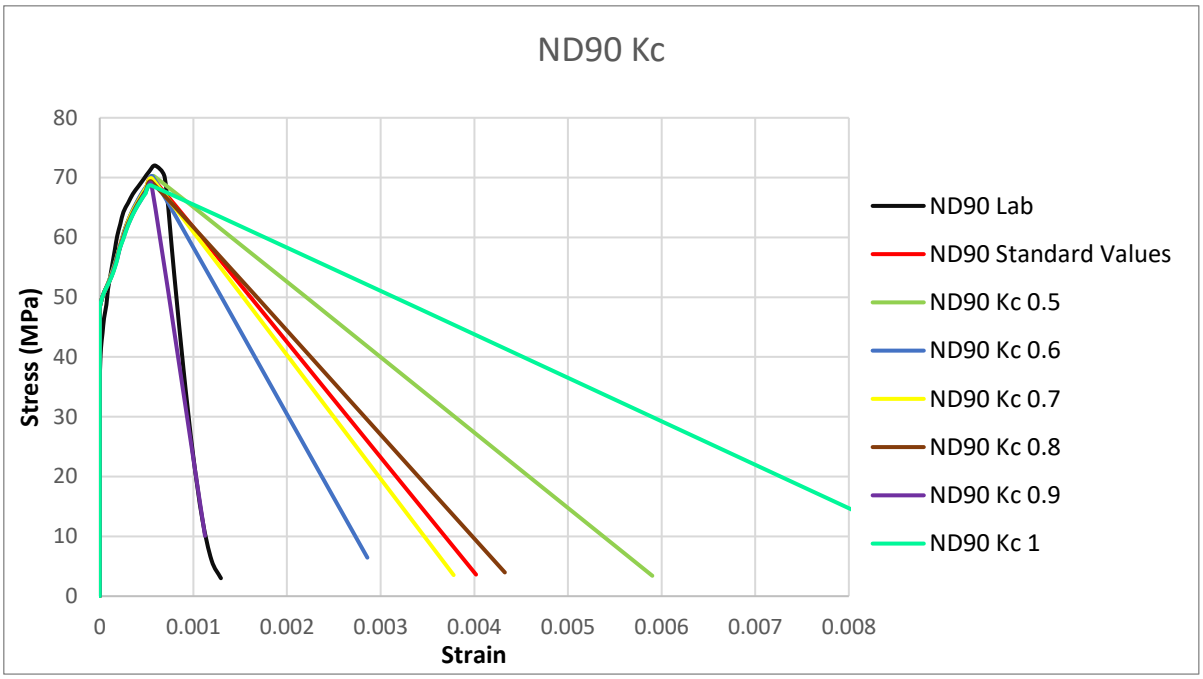

Figure 42: ND90 Kc

To be noted here is how an increased value of Kc, nearly at its upper limit value, yielded a desirable result with the stronger, more brittle concrete type – while for ND55, as high of a Kc-value would yield an invalid result.

4.5.6. C90 Viscosity parameter

While there were no convergence issues with the simulation (the analyses had no problem running their full course), a slight change in behaviour was observed when implementing a minor viscosity value of 0.0001. A more steep curve, closer in similarity to the experimental results, was observed – yet including the linear behaviour that has troubled the ND90-results.

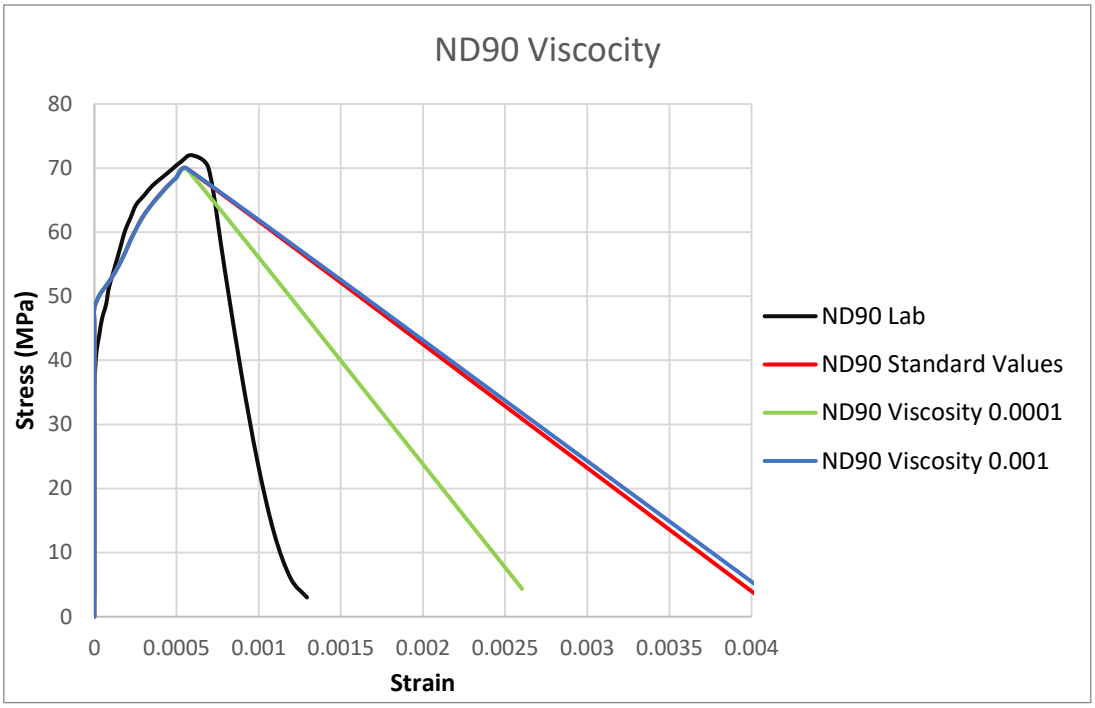

Figure 43: ND90 Viscosity parameter

4.5.7. C90 Parameter combinations

Given that the ND90 Cylinder testing has proven itself limited in terms of recreation capabilities, attempts at combining parameters to optimise the resulting curves have been unsuccessful. Utilising a combination of increased Fb0/Fc0-values and a non-zero value of the viscosity parameter showed some promise when added together with some of the dilation angles that was found to be better, but clear deviances from the laboratory results still remained.

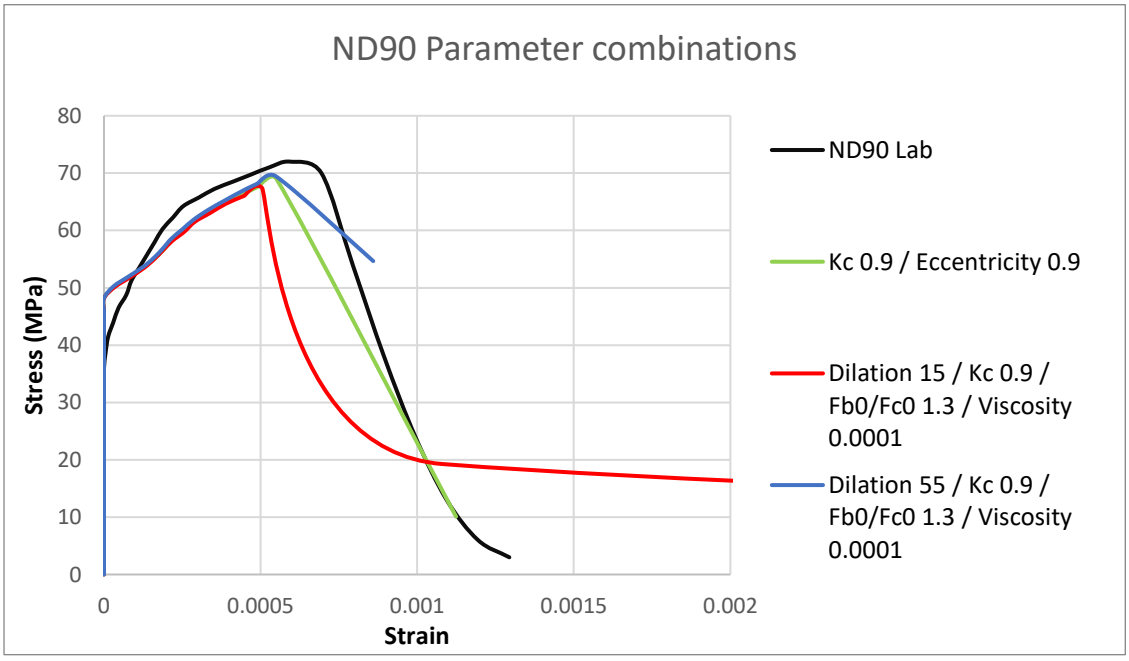

Figure 44: ND90 Parameter Optimisation

4.6. Beam tests (*"B25/55/90"*)

Following the cylinder testing, a limited beam testing phase was conducted. Using the setup as described in chapter 3, a few results were extracted to be considered for this research. The results of the beam tests were taken out as Force-Displacement curves over time, from there the displacements are calculated to compressive strain with the following formula:

$$Strain = \frac{\Delta L}{L} \qquad \text{Eq. 31}$$

The test was done for the over-reinforced concrete for each of the concrete types in the cylinder tests. Figure 45 shows the Load-Compressive strain curvature from Markeset [3], and an as accurate as possible recreation to use for data comparison for the results.

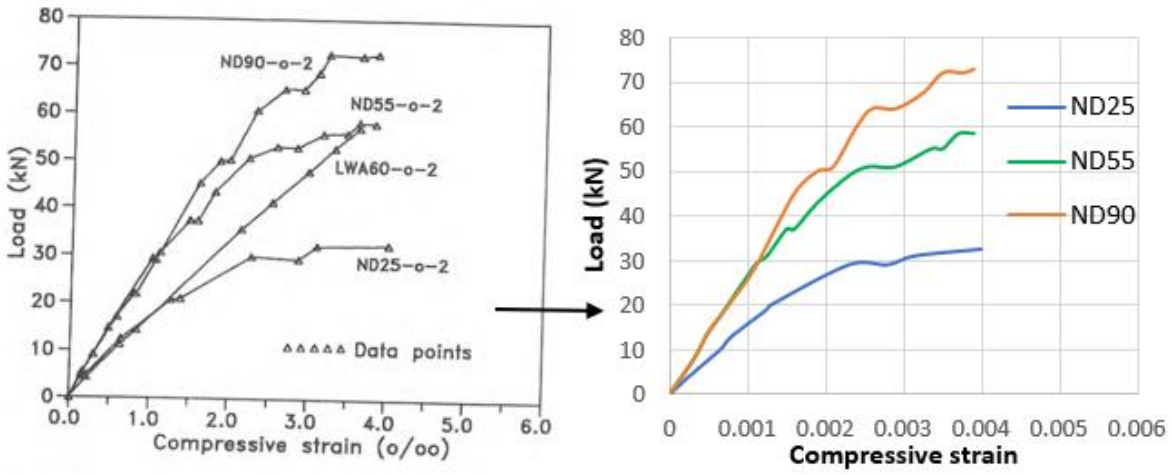

Figure 45: Load-compressive strain curve for over-reinforced beams from Markeset (left, [3]) translated in plotting software to be used for data comparison (right).

4.6.1. B25

Analyses with standard and "optimal" parameters were performed to observe how the uniaxial testing data from the concrete cylinder results translated to a beam bending problem.

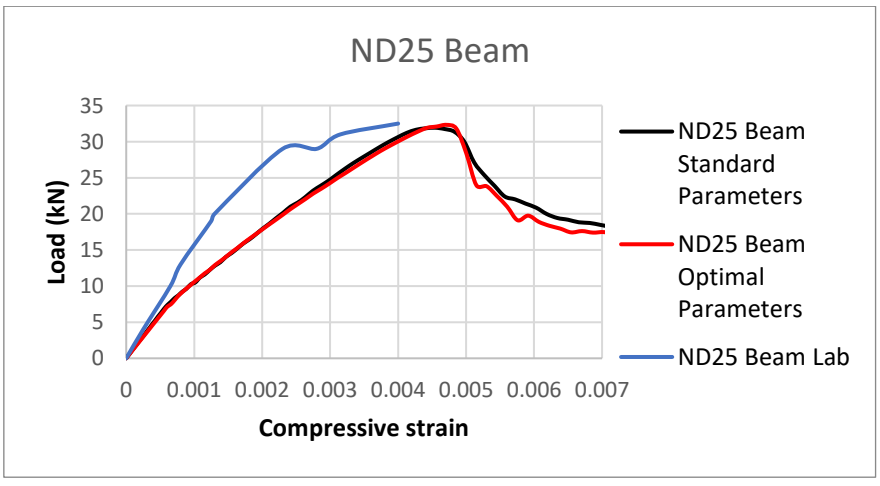

Figure 46: ND25 Beam test results

The beam with ND25 concrete shows somewhat positive results compared to the laboratory tests as they seem to have similar maximum load P_{max}. Deviance from the experimental result was observed, with both parameter tests struggling to match the laboratory Load-Strain curve.

As the different parameters didn't seem to affect the elastic part of the beam tests, only the softening curve, there was not much information gathered from the parameter comparison when the beam was considered.

4.6.2. B55

Same procedure for ND55, where the optimal and standard parameters were tested to see if they had an impact on the beam results.

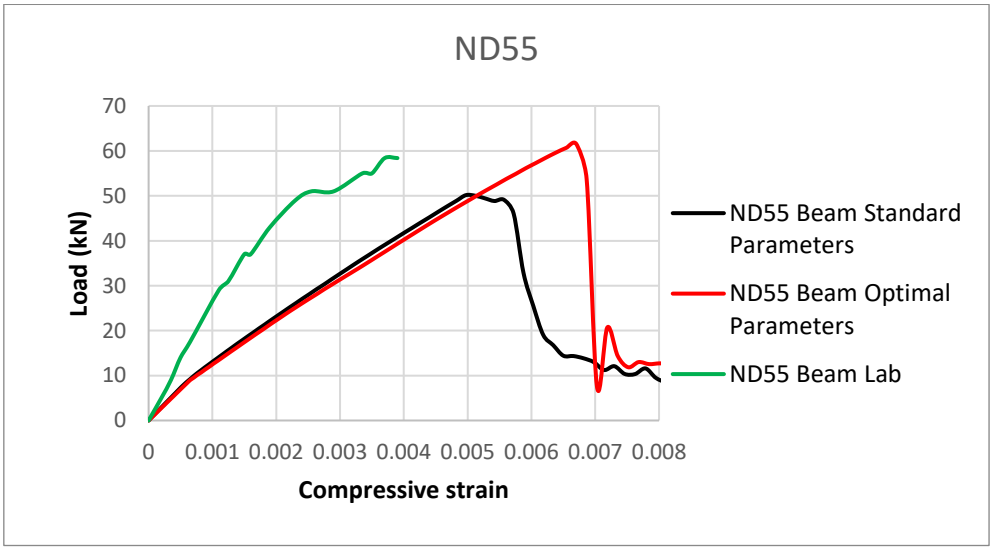

Figure 47: ND55 Beam test results

The optimal parameters for the cylinder tests resulted in a higher P_{max} than the standard parameters, a clear difference between the two parameter sets. The optimised parameter post-yield data exhibits significantly increased brittle behaviour when compared to the standard parameter test, while the maximum load appear more akin to the experimental results. The same issue occurred for ND55 as with ND25 when the elastic part was compared as they strayed even more from the ideal curve.

4.6.3. B90

The ND90 Beam test was a clear deviant from the rest of the analyses, as illustrated by Figure 48. The results for the ND90 are not similar in any remarks as the elastic part and P_{max} is far apart. The post-yield result is also considered invalid due to its irregular behaviour.

As the results for the cylinder wasn't usable it is no surprise that the beam also encountered problems. The elastic part is similar to both ND25 and ND55 in a way that they all have a more gradual slope than their corresponding laboratory tests.

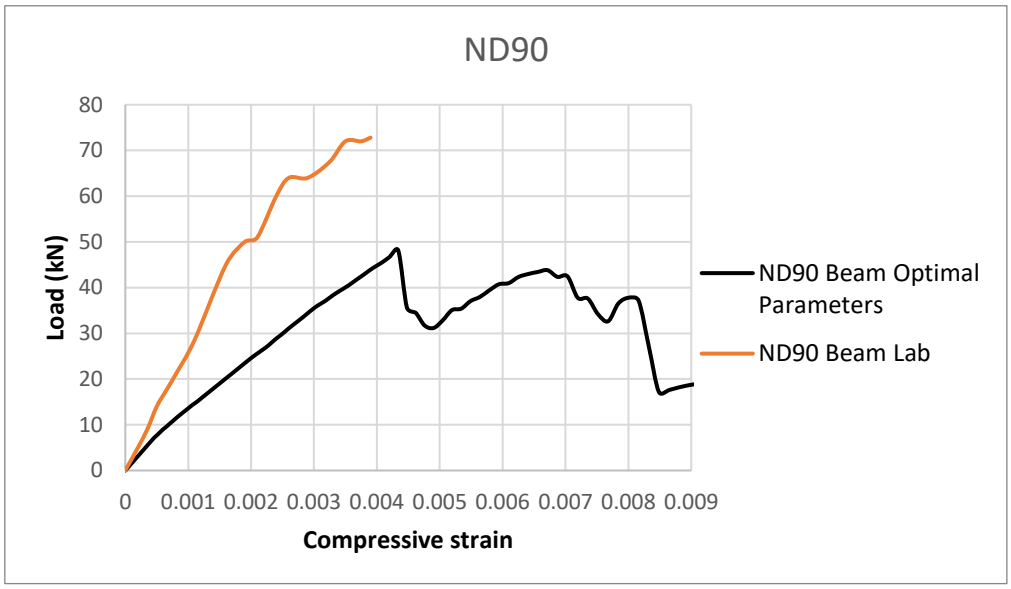

Figure 48: ND90 Beam test results

5. Discussion

Following the numerical modelling and sensitivity study of CDP, this chapter will discuss the effects observed when altering the input data and parameters of the concrete model. It is relevant to consider the effect that the various parameters have on simulations for the uniaxial compression scenario as well as the beam bending problem, in order to be able to draw conclusions regarding the validity of utilising CDP for the specific problems that this thesis presents.

It will also be relevant to consider the relevancy and overall validity of the data gathered, and to weigh this up against the research questions as presented in the introduction of this thesis.

5.1. Uniaxial analyses

A thorough uniaxial analyses have been conducted on a concrete cylinder with different concrete types. At the three concrete types provided, different parameters were tested in an attempt to find the best suitable result compared to a laboratory test provided by Markeset [3].

The result obtained indicates the given concrete's characteristics and how they compare to the recommended parameters suggested by Abaqus. Some of the values are somewhat dependent on each other and should therefore be altered in correspondence to each other (Kc, eccentricity, and dilation angle). However, in this thesis the objective has been to replicate the stress-strain curve as best as possible without going outside reasonable parameters.

In the Uniaxial tests a change in the eccentricity parameter did not impact the stress-strain curve. When a combination of suitable parameters was preformed both Kc and dilation angle was changed as the combination of these parameters led to similarities between the Abaqus output and the laboratory results.

Even though there was no intention to change Kc and dilation angle together as a mean to satisfy the theory behind the parameter, the result ended up being in accordance with the theory as that presented the best stress-strain resemblance.

5.1.1. ND25 Cylinder

As a result of the parameter testing, it is shown that recommended parameters did not perform the best for the ND25 cylinder. Rather a dilation angle of 15, Kc value of 0.9 and a Fb0/Fc0 ratio of 1 had the best outcome.

These parameters together would suggest that this concrete is more brittle than what the parameter suggested is intended for. This is also represented well in the stress-strain curves procured as the softening curve is a bit steeper.

As the dilation angle and KC value is connected and is the main contributors to change in the stress-strain curve it would be realistic to assume that another combination of these values could give similar results.

There was rarely any case where the ND25 cylinder encountered problems where the softening curve got a linear behaviour as a result of lack in points along the curve. Therefore, the authors were more free in testing the parameters in addition to different load settings. These changes did not contribute to any remarkable changes despite maybe a higher max strain as the stress would never reach zero. This is not included in the paper as there were nothing to compare it to and it was regarded as insignificant manipulations of the results.

The element type C3D8R instead of C3D8 yielded adequate results; Reduced integration was acceptable with this concrete type, as it did not lead to any problems in the results or with the analysis.

5.1.2. ND55 Cylinder

ND55 encountered some issues during the parameter testing as there were no values gathered between the ultimate stress and a stress value at 0 for the softening curve. However, a solution was found for this problem after some testing and tinkering in the program. The solution found was to change the element type to C3D8 instead of the C3D8R, the only change is that there is no reduced integration.

A reason for this might be because the reduced integration only uses a single integration point in the centre of an element and not multiple at the corners of an element, [41]. This resulted in a difference from 1 to 8 integration points for the output. Therefore, it is concluded that its highly likely that the reduces integration overlooks values in the critical sone.

Another possible solution was to ask for more detailed output when there is not registered any points in the analysis. This was not successful as the result turned out to be the same, even though the output was altered to obtain a hundred times more datapoints.

As the solution of C3D8 worked it was possible to find the best suitable parameters for ND55. It was found that a dilation angle of 25 and a Kc value of 0.7 was optimal, which would indicate that this concrete also is more brittle than what the recommended parameters is suggested for. In this case it was not possible to combine a Fb0/Fc0 ratio of 1 with the other changes as the problem discussed with a linear softening curve would occur.

5.1.3. ND90 Cylinder

ND90 encountered the same problem that ND55 did, but unfortunately there were not found a solution for this concrete. The authors tested several mesh types to see if it could be a problem in the same nature as ND55, but with no luck. A wide range of load changes was also tested with no luck.

An assumption could be made in order to make an educated guess on which parameters would suit ND90. If the results for ND25 and ND55 is assumed to relate to the ND90 result it would make sense that the dilation angle would increase a bit and the Kc value would decrease. If this assumption is faceable the ND90 properties would be fairly similar to the recommended parameters.

By assessing Figure 38: ND90 Baseline test it seems plausible, with an ultimate stress that is fairly similar and not much else to evaluate it could be possible. However, the elastic segment of the curve is also off by a bit. But this can be excused by the lack of input

parameters. The validation of ND90 is still lacking as no real result can be obtained in the analyses.

5.1.4. Cylinder summary

Two of the three concrete types showed promising result in uniaxial analyses of the cylinders, with ND25 and ND55 giving close to ideal curves when compared to their corresponding laboratory tests when right parameters are used. For ND90 the case is unfortunately that the results should mostly be overlook as the analysis didn't provide realistic results.

5.2. Beam analyses

Following a set of partially successful cylinder analyses, observing satisfactory results for both concrete quality ND25 and ND55, the beam analyses require a certain scepticism when considering the nature of CDP, uniaxial compressive testing and the difference related to a beam in bending.

The most important aspect to compare between the cylinder and beam analyses is the raw effect of transferring uniaxial test data to the beam problem, without any general applications of strain gradient and localisation effect in the compressive zone. Observing the effect of the recommended standard parameter values versus the "optimised" values for cylindrical tests is also of interest to investigate, while observing the deviancy from the experimental Load-Compressive strain results that is present in all beam results.

The results from the beam analyses are presented as Load-Compressive strain curves in order to gain the best comparative base between experimental test and Abaqus analysis. By extracting the displacements in the compressive zone of the beams, it is possible to convert the results to compressive strain values.

5.2.1. ND25 Beam

The ND25 beam results can be considered the most valid of the three beam types, having the least deviancy from the experimental data. The analyses peak load is similar to the experimental data, while the post-yield behaviour is brittle; Shortly after ultimate stress is achieved, the curves display failure and softening occurs swiftly, as opposed to the experimental ND25 data which has a long strain hardening zone before data recording stops.

When considering the behaviour of the ND25 beam, considering the theory about strain gradients and localisation is important. As one would expect to observe relatively ductile behaviour when utilising the ND25 data, the analysis of the ND25 beam underlines the general lack of localisation in the CDP model which impacts the results correspondingly. The optimised uniaxial properties of the ND25 cylinder exhibits a clear lack of transferability to the beam problem, confirming what the theory suggests about brittleness vs. ductility expectations.

When considering the difference between standard parameter and optimised values from the cylinder test, these is not much deviance to observe. This could be a suggestion towards general applicability of optimised values on the beam model, should the initial difference between the experimental and numerical tests be possible to minimise.

There is a possibility that introducing a strain gradient regime for the compressive zone of the concrete will create more desirable results with more ideal ductility properties, however this is beyond the scope that this research covers.

5.2.2. ND55 Beam

Considering the beam with ND55 concrete properties, the analyses begin to deviate severely. The difference between the experimental data and the analyses results has become so great that the analysis data cannot be considered representative of the experiments from the lab.

Using the optimal data from the cylinder tests yields heightened peak load and strain data, deviating to nearly double the strain of the experiment. Post-yield is observed as highly brittle, with a near instant failure following the ultimate load. The analysis data is considered completely anomalous from its experimental counterpart.

The standard parameter values yield a result with less sudden post-yield softening behaviour but is still considered far from acceptable. Both analysis results seem to behave much too linear in the elastic/early hardening zone, which might be related to issues within the software with the input data and could also relate to the lack of gradient parameters for the concrete.

5.2.3. ND90 Beam

Introducing the already faulty ND90 cylinder data to the ND90 beam model proved itself to be just as problematic as expected. Irregular stress-load behaviour after failure hints towards computational problems. The ND90 beam data cannot be considered representative to any credible result, as the data simply does not appear reliable.

A brief investigation into the load time of the beam indicates the presence of dynamic behaviour (vibrations and fluctuations) that appear as the load is applied, as well as a heavy dependency to material density. While this is not presented in the results, the authors find it relevant to mention this a possible focus point for any future attempt at continuing the research presented.

5.2.4. Beam summary

In summary of the 3 different beam analyses that was conducted in this thesis, it is difficult to suggest that the data results presented can be considered reliable without further analyses and possibly implementation of further parameters in the Abaqus subroutines.

5.3. Concrete Damaged Plasticity in Abaqus FEA

The CDP model as it is implemented in Abaqus FEA can be considered a good tool for modelling concrete: Previous research confirms this, and parts of this thesis reinforces that belief – however, it should not go unmentioned that the common occurrence of implementing custom registries in the Abaqus subroutine points towards a general lack of certain details that are needed for accurate analysis of various concrete structures. The brief list of previous research presented in chapter 2.9, combined with the various sources presented in the thesis, clearly indicates that while CDP offers a good baseline for concrete modelling, many applications require more specialised modelling parameters than what CDP can offer.

5.4. Sources of error and general shortcomings

When it comes to numerical modelling and non-linear analysis, the occurrence of errors is always necessary to consider. Abaqus FEA as a modelling software is a precision tool appreciated by various special construction departments worldwide, so dismissing the capabilities of the software would be naïve.

Abaqus/Explicit is a sensitive tool for nonlinear analysis, and it almost easier to implement a problem by using the wrong settings than it is to achieve good and credible results. In order to achieve as little uncertainty with the program as possible, careful implementation of the different settings of Abaqus FEA had to be performed. Most input settings utilised in this thesis are standard for most applications, and the authors have been careful to make use of similar properties to those used in other courses and projects throughout their master's programme.

With permission from the thesis supervisor, the authors reached out to an individual (who wished to remain anonymous) with broad experience with Abaqus in order to discuss the overall settings of the software. While they were unable to provide guidance with the CDP model itself, having them validate the base setup of the models has proved invaluable. This is where it is important for the authors to point out that the lack of guidance with the CDP model itself introduces a possible source of error.

While general confidence in the application of the model remains high, it would appear arrogant to assume that there are no settings within Abaqus/Explicit in combination with CDP that can be tweaked and optimised. This should be considered a significant area to search for improvements if attempting to continue the beam analyses scenario.

Another important source of error to discuss is the presence of the issues presented in detail in chapter 4.5 ND90 Cylinder. The authors suspect the linear behaviour as discussed in the results may be a combination of ill-fitting input data and a potential to change some analysis settings. The discovery that reduced integration significantly improved data results for ND25 and ND55, and the fact that this did not transfer to the ND90 simulations opens up the possibility that altering the integration method in combination with certain other aspects of the FEA tool may improve results considerably. This was certainly not investigated in enough detail in this research, and settings like reduced load speed, introduction of ramped loading, and/or super-fine meshing could possibly be part of a solution to optimise the compressive cylinder tests for the ND90 concrete.

While this thesis has investigated the application of CDP in Abaqus/Explicit, there is an argument to be made that Abaqus/Standard may work better for this specific scenario. While this research was focused on the application of the explicit solver, the beam analysis revealed that this solution method may introduce dynamic anomalies like those observed in the ND90 beam results. While some advantages were identified as presented in chapter 2.6.10, the authors will not dismiss the possibility that sacrificing these advantages to attempt analyses in Abaqus/Standard could yield considerable results.

6. Conclusive remarks and further work

The overall purpose of this work was to investigate the Concrete Damaged Plasticity model in Abaqus FEA, utilising the Abaqus/Explicit solver in order to simulate experimental data provided to the authors through a previous study. In an attempt to answer the presented research questions, the authors have looked into the core theory of CDP and applied the parameter theory of the model to the FEA software.

"To which extent is it possible to extract the data from an experimental study on uniaxial concrete compressive testing, recreating the test cylinders as finite element models in Abaqus FEA and simulate the results using Concrete Damaged Plasticity?"

The authors have presented results showcasing that it is possible to take the uniaxial compressive test data for cylinders and use this to model and simulate the cylinder experiment in Abaqus FEA with CDP, with some limitations when regarding higher strength/increased brittleness concrete. As such, the first research question is answered in part and the authors have confidence in that further work will make it possible to accurately recreate the ND90 cylinder results.

"How representative are the results from running a non-linear finite element analysis of an over-reinforced concrete beam subjected to 4-point bending, when using the values for uniaxial compressive material tests and the results of uniaxial cylinder compressive tests?"

"To which degree can the parameter values that are determined in the sensitivity study of the cylinder tests be transferred to the beam-problem?"

The results indicate that a lot of work remain in order to successfully recreate the beam tests from the experiment, and the authors have addressed possible errors and shortcomings that may help in improving these results. As presented through a limited study of the beam models, it is not adequate to simply translate the uniaxial test data to the beam model without further adapting CDP in Abaqus FEA settings.

"What are the challenges when attempting to translate uniaxial compressive test values to a beam bending problem? Will the presence of gradient strains and the phenomena of localisation in an over-reinforced concrete beam be a problem for the Concrete Damaged Plasticity model in Abaqus FEA?"

The discussion of this thesis addresses some the issues identified relating to the beam analyses. It is highly relevant to consider the common practise of implementing additional subroutines in Abaqus FEA in order to achieve desired results: An indication of Abaqus FEA and CDP's more general-purpose applicability. In order to solve various specific scenarios, more than simply working with the barebone CDP model is required in order to achieve high accuracy results.

Additionally, the lack of customisability when regarding compressive strain gradients and localisation in CDP's raw form makes it difficult to rely on the reinforced concrete beam cases. Again, the common presence of custom-made user subroutines points towards the complex nature of concrete modelling, and the following requirements in knowledge when it comes to Finite Element Modelling and Analysis.

Considering the work presented in this thesis, the authors wish to recommend further work that can be considered as part of better understanding the complex nature of this modelling scenario. These are paths that were not possible to be covered in this research.

- In general, a more extensive look into the Abaqus software itself and the settings that follow with the use of CDP may help solve issues discussed in this thesis.
- It should be relevant to consider the implementation of gradient/localisation data, in order to cover the lack of ductile behaviour of the beam models. For instance, implementing simple subroutines may prove significant in optimising this work.
- The research presents an opportunity for cross-disciplinary work on the CDP model, where implementation of scripts (e.g., Python-codes) combined with a structural and material base could allow for the creation of a CDP model more suited for the scenario as presented.
- Using the work that this thesis presents, it could prove useful to conduct a series of new experiments where most, if not all, of the relevant input parameters are determined using uni-, bi- and/or triaxial laboratory testing.
- Following the previous suggestion, an argument can be made that cyclic (load-unload) and tensile testing would also make for a useful basis for a more in-depth analysis of CDP.

Reference list

1. Sørensen, S.I., *Betongkonstruksjoner*. 2013, no: Akademika. 470 s. fig.
2. Polus, Ł. and M. Szumigała, *Laboratory tests vs. FE analysis of concrete cylinders subjected to compression.* AIP Conference Proceedings, 2019. **2078**(1): p. 020089.
3. Markeset, G., *Failure of Concrete under Compressive Strain Gradients*, in *Department of Structural Engineering*. 1993, Norwegian Institute of Technology: Trondheim, Norway.
4. Silva, L.M.E., A.L. Christoforo, and R.C. Carvalho, *Calibration of Concrete Damaged Plasticity Model parameters for shear walls.* Matéria (Rio de Janeiro), 2021. **26**(1).
5. StandardNorge, *Eurocode: Basis of structural design*. 1990-2016.
6. Koutromanos, I., *Fundamentals of Finite Element Analysis: Linear Finite Element Analysis*. 2018, United Kingdom of Great Britain and Northern Ireland: Wiley.
7. Kim, N.-H., *Introduction to Nonlinear Finite Element Analysis*. 1. ed. 2015, New York, USA: Springer New York.
8. Cook, R.D.M., D. S. ; Plesha, M. E. ; Witt, R. J., *Concepts and applications of finite element analysis - 4th edition*. 4. ed. 2002, United Kingdom: Wiley.
9. Raymond Ian Gilbert, N.C.M., Gianluca Ranzi, *Design of Prestressed Concrete to Eurocode 2*. 2. ed. 2017, Boca Raton, FL: CRC Press.
10. Anam, I. and Z. Shoma, *NONLINEAR PROPERTIES OF REINFORCED CONCRETE STRUCTURES*. 2002.
11. Labuz, J.F. and A. Zang, *Mohr–Coulomb Failure Criterion.* Rock Mechanics and Rock Engineering, 2012. **45**(6): p. 975-979.
12. Coulomb, C., *ESSAI SUR UNE APPLICATION DES REGLES DE MAXIMIS ET MINIMIS A QUELQUES PROBLEMES DE STATIQUE RELATIFS A L'ARCHITECTURE (ESSAY ON MAXIMUMS AND MINIMUMS OF RULES TO SOME STATIC PROBLEMS RELATING TO ARCHITECTURE).* Acad Sci Paris Mem Math Phys, 1776. **7.**: p. 343-382.
13. Mohr, O., *Welche Umstände bedingen die Elastizitätsgrenze und den Bruch eines Materials?* Zeitschrift des Vereines deutscher Ingenieure, 1900. **44**(45): p. 1524-1530.
14. Drucker, D.C. and W. Prager, *SOIL MECHANICS AND PLASTIC ANALYSIS OR LIMIT DESIGN.* Quarterly of Applied Mathematics, 1952. **10**(2): p. 157-165.
15. Mises, R.v., *Mechanik der festen Körper im plastisch- deformablen Zustand [Mechanics of Solid Bodies in Plastic Deformation State].* Nachrichten von der Gesellschaft der Wissenschaften zu Göttingen, Mathematisch-Physikalische Klasse, 1913. **1913**(1.).
16. SIMULIA. *Abaqus Analysis User's Guide.* [cited 2023 23.01]; Available from: https://classes.engineering.wustl.edu/2009/spring/mase5513/abaqus/docs/v6.6/books/usb/default.htm.
17. SIMULIA. *Abaqus Theory Guide.* [cited 2023 23.01]; Available from: https://classes.engineering.wustl.edu/2009/spring/mase5513/abaqus/docs/v6.6/books/stm/default.htm.
18. SIMULIA. *Abaqus Keywords Reference Guide.* [cited 2023 23.01]; Available from: https://classes.engineering.wustl.edu/2009/spring/mase5513/abaqus/docs/v6.6/books/key/default.htm.
19. Lubliner, J., et al., *A Plastic-Damage Model for Concrete.* International Journal of Solids and Structures, 1989. **25**(3): p. 299-326.
20. Lee, J.H. and G.L. Fenves, *Plastic-damage model for cyclic loading of concrete structures.* Journal of Engineering Mechanics-Asce, 1998. **124**(8): p. 892-900.
21. Alejano, L. and A. Bobet, *Drucker–Prager Criterion.* Rock Mechanics and Rock Engineering, 2012. **45**: p. 995-999.
22. Bathe, K.-J., et al., *Nonlinear analysis of concrete structures.* Computers & Structures, 1989. **32**(3-4): p. 563-590.

23. Tavarez, F.A. and M.E. Plesha, *Discrete element method for modelling solid and particulate materials*. International Journal for Numerical Methods in Engineering, 2007. **70**(4): p. 379-404.
24. Tu, Z. and Y. Lu, *Evaluation of typical concrete material models used in hydrocodes for high dynamic response simulations*. International Journal of Impact Engineering, 2009. **36**(1): p. 132-146.
25. Rakic, D., et al., *CONCRETE DAMAGE PLASTICITY MATERIAL MODEL PARAMETERS IDENTIFICATION*. Journal of the Serbian Society for Computational Mechanics, 2021. **15**: p. 111-122.
26. Malm, R., *Shear cracks in concrete structures subjected to in-plane stresses*. 2006.
27. Duvaut, G.L., J. L., *Les inequations en mecanique et en physique*. 1972, Travaux et recherches mathématiques, Paris: Dunod.
28. Wosatko, A., J. Pamin, and M.A. Polak, *Application of damage–plasticity models in finite element analysis of punching shear*. Computers & Structures, 2015. **151**: p. 73-85.
29. Francis, P., *The influence of shear connection strength and stiffness on the resistance of steel-concrete composite sandwich panels to out-of-plane forces*, G. Parke, et al., Editors. 2020, University of Surrey.
30. Hillerborg, A., M. Modéer, and P.E. Petersson, *Analysis of crack formation and crack growth in concrete by means of fracture mechanics and finite elements*. Cement and Concrete Research, 1976. **6**(6): p. 773-781.
31. J. Červenka, V.Č., S. Laserna, *On crack band model in finite element analysis of concrete fracture in engineering practice*. Elsevier Engineering Fracture Mechanics, 2018. **197**: p. 27-47.
32. Zhang, Y., et al., *A simple implementation of localizing gradient damage model in Abaqus*. International Journal of Damage Mechanics, 2022. **31**(10): p. 1562-1591.
33. BV, D.F. *DIANA-10.1 User's Manual - Material Library*. 2017 [cited 2023 07.04]; First Edition:[Available from: https://manuals.dianafea.com/d101/MatLib/node226.html.
34. Environment, R.-M.o.I.a.t., *Guidelines for Nonlinear Finite Element Analysis of Concrete Structures*. 2017.
35. Cervenka, J. and V. Cervenka, *On the uniqueness of numerical solutions of shear failure of deep concrete beams: Comparison of smeared and discrete crack approaches*. Computational Modeling of Structures, EURO-C 2010, 2010: p. 281-290.
36. Feenstra, P.H., *Computational Aspects of Biaxial Stress in Plain and Reinforced Concrete*, in *Civil Engineering and Geosciences*. 1993, Delft University of Technology.
37. Hafezolghorani Esfahani, M., et al., *Simplified Damage Plasticity Model for Concrete*. Structural Engineering International, 2017. **27**: p. 68-78.
38. Szczecina, M. and A. Winnicki. *Calibration of the CDP model parameters in Abaqus*. 2015.
39. Wang, Q., et al., *Study on concrete damaged plasticity model for simulating the hysteretic behavior of RC shear wall*. IOP Conference Series: Materials Science and Engineering, 2020. **789**: p. 012065.
40. Fedoroff, A. and K. Calonius, *Using the Abaqus CDP model in impact simulations*. Rakenteiden Mekaniikka, 2020. **53**: p. 180-207.
41. SIMULIA. *Getting Started with ABAQUS/Standard: Keywords Version*. [cited 2023 23.05]; Available from: https://classes.engineering.wustl.edu/2009/spring/mase5513/abaqus/docs/v6.5/books/gss/default.htm?startat=ch04s01.html.

Appendices

CDP material input tables

ND25

Concrete material overview: Modelling inputs			
Concrete type: ND25		Plasticity parameters	
		Dilation angle	35
Elastic properties		Eccentricity	0.1
Young's modulus (GPa)	20.1	Fb0/fc0	1.16
Poisson's Ratio	0.2	Kc	2/3
		Viscosity	0.0001
Compressive properties		Compressive damage	
Yield stress (MPa)	Inelastic strain	Damage parameter, dc	Inelastic strain
5	0	0	0
9	5.22388E-05	0	5.22388E-05
12.5	0.000128109	0	0.000128109
16	0.00020398	0	0.00020398
19	0.000304726	0	0.000304726
21.5	0.000430348	0	0.000430348
22	0.000655473	0	0.000655473
22.2	0.000895522	0	0.000895522
20	0.001254975	0.099099099	0.001254975
18.5	0.001579602	0.166666667	0.001579602
17.2	0.001894279	0.225225225	0.001894279
16	0.00220398	0.279279279	0.00220398
15	0.002503731	0.324324324	0.002503731
14	0.002803483	0.369369369	0.002803483
13	0.003103234	0.414414414	0.003103234
12	0.003402985	0.459459459	0.003402985
11	0.003702736	0.504504505	0.003702736
10	0.004002488	0.54954955	0.004002488
9	0.004302239	0.594594595	0.004302239
8	0.00460199	0.63963964	0.00460199
7	0.004901741	0.684684685	0.004901741
6	0.005201493	0.72972973	0.005201493
5	0.005751244	0.774774775	0.005751244
4	0.006050995	0.81981982	0.006050995
3	0.006350746	0.864864865	0.006350746
2	0.006650498	0.90990991	0.006650498
1	0.006950249	0.954954955	0.006950249
Tensile properties		Tensile damage	
Yield stress (MPa)	Cracking strain	Damage parameter, dt	Cracking strain
3.6	0	0	0
2.94	8.65513E-05	0.183333333	8.65513E-05
2.25	0.00025519	0.375	0.00025519
1.94	0.000386273	0.461111111	0.000386273
1.62	0.000517853	0.55	0.000517853
1.08	0.000871349	0.7	0.000871349
0.73	0.001106592	0.797222222	0.001106592
0.5	0.005129264	0.861111111	0.005129264

ND55

Concrete material overview: Modelling inputs			
Concrete type: ND55		Plasticity parameters	
		Dilation angle	35
Elastic properties		Eccentricity	0.1
Young's modulus (GPa)	23.9	Fb0/fc0	1.16
Poisson's Ratio	0.2	Kc	2/3
		Viscosity	0.0001
Compressive properties		Compressive damage	
Yield stress (MPa)	Inelastic strain	Damage parameter, dc	Inelastic strain
5.5	0	0	0
11	3.9749E-05	0	3.9749E-05
16	8.05439E-05	0	8.05439E-05
21	0.000121339	0	0.000121339
25	0.000203975	0	0.000203975
30	0.00024477	0	0.00024477
35	0.000285565	0	0.000285565
39	0.000368201	0	0.000368201
44	0.000408996	0	0.000408996
45.3	0.000714603	0	0.000714603
40	0.00107636	0.116997792	0.00107636
37	0.001451883	0.183222958	0.001451883
32	0.001911088	0.293598234	0.001911088
29	0.002286611	0.3598234	0.002286611
26	0.002662134	0.426048565	0.002662134
21	0.003121339	0.536423841	0.003121339
19	0.003455021	0.580573951	0.003455021
17	0.003788703	0.624724062	0.003788703
13	0.004206067	0.713024283	0.004206067
11	0.004539749	0.757174393	0.004539749
9	0.004873431	0.801324503	0.004873431
7	0.005207113	0.845474614	0.005207113
5	0.005540795	0.889624724	0.005540795
3	0.005874477	0.933774834	0.005874477
1	0.006208159	0.977924945	0.006208159
Tensile properties		Tensile damage	
Yield stress (MPa)	Cracking strain	Damage parameter, dt	Cracking strain
3.6	0	0	0
2.94	8.65513E-05	0.183333333	8.65513E-05
2.25	0.00025519	0.375	0.00025519
1.94	0.000386273	0.461111111	0.000386273
1.62	0.000517853	0.55	0.000517853
1.08	0.000871349	0.7	0.000871349
0.73	0.001106592	0.797222222	0.001106592
0.5	0.005129264	0.861111111	0.005129264

ND90

Concrete material overview: Modelling inputs			
Concrete type: ND90		Plasticity parameters	
		Dilation angle	35
Elastic properties		Eccentricity	0.1
Young's modulus (GPa)	26.5	Fb0/fc0	1.16
Poisson's Ratio	0.2	Kc	0.6667
		Viscosity	0
Compressive properties		Compressive damage	
Yield stress (MPa)	Inelastic strain	Damage parameter, dc	Inelastic strain
51.25	0	0	0
53.5	0.000112411	0	0.000112411
55.75	0.000137232	0	0.000137232
58	0.000162053	0	0.000162053
60.25	0.000186874	0	0.000186874
62.25	0.000220048	0	0.000220048
64.25	0.000253222	0	0.000253222
65.75	0.000303103	0	0.000303103
67.25	0.000352983	0	0.000352983
68.5	0.000411217	0	0.000411217
69.75	0.000469451	0	0.000469451
71	0.000527685	0	0.000527685
72	0.000594272	0	0.000594272
70	0.000761098	0.027777778	0.000761098
54	0.001395704	0.25	0.001395704
38	0.00203031	0.472222222	0.00203031
24	0.002598091	0.666666667	0.002598091
13	0.003065632	0.819444444	0.003065632
6	0.003399523	0.916666667	0.003399523
3	0.003599761	0.958333333	0.003599761
1.75	0.003741527	0.975694444	0.003741527
1	0.003866587	0.986111111	0.003866587
0.4	0.003986635	0.994444444	0.003986635
Tensile properties		Tensile damage	
Yield stress (MPa)	Cracking strain	Damage parameter, dt	Cracking strain
3.6	0	0	0
2.94	8.65513E-05	0.183333333	0.0000866
2.25	0.00025519	0.375	0.00025519
1.94	0.000386273	0.461111111	0.000386273
1.62	0.000517853	0.55	0.000517853
1.08	0.000871349	0.7	0.000871349
0.73	0.001106592	0.797222222	0.001106592
0.5	0.005129264	0.861111111	0.005129264

List of performed simulations in Abaqus:

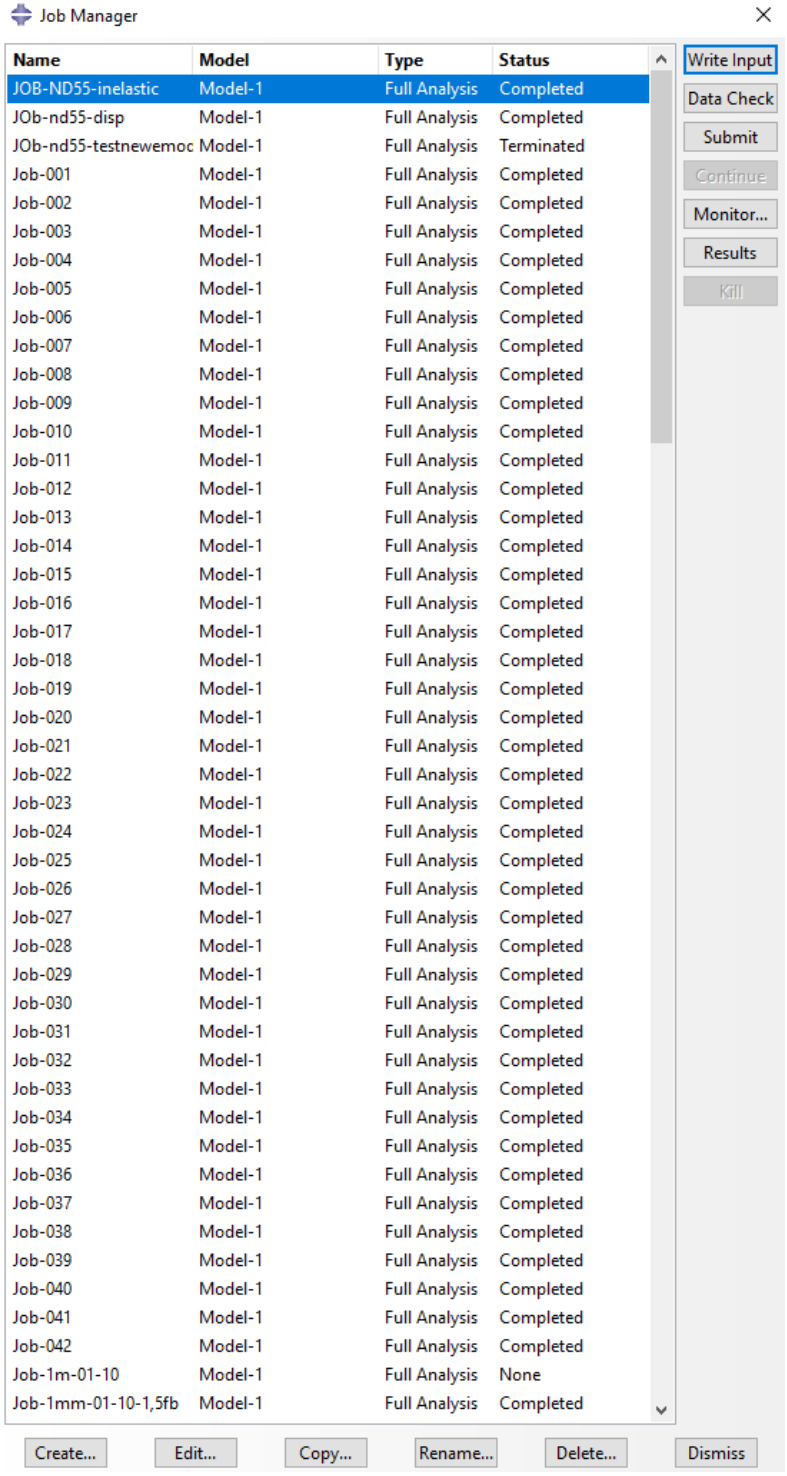

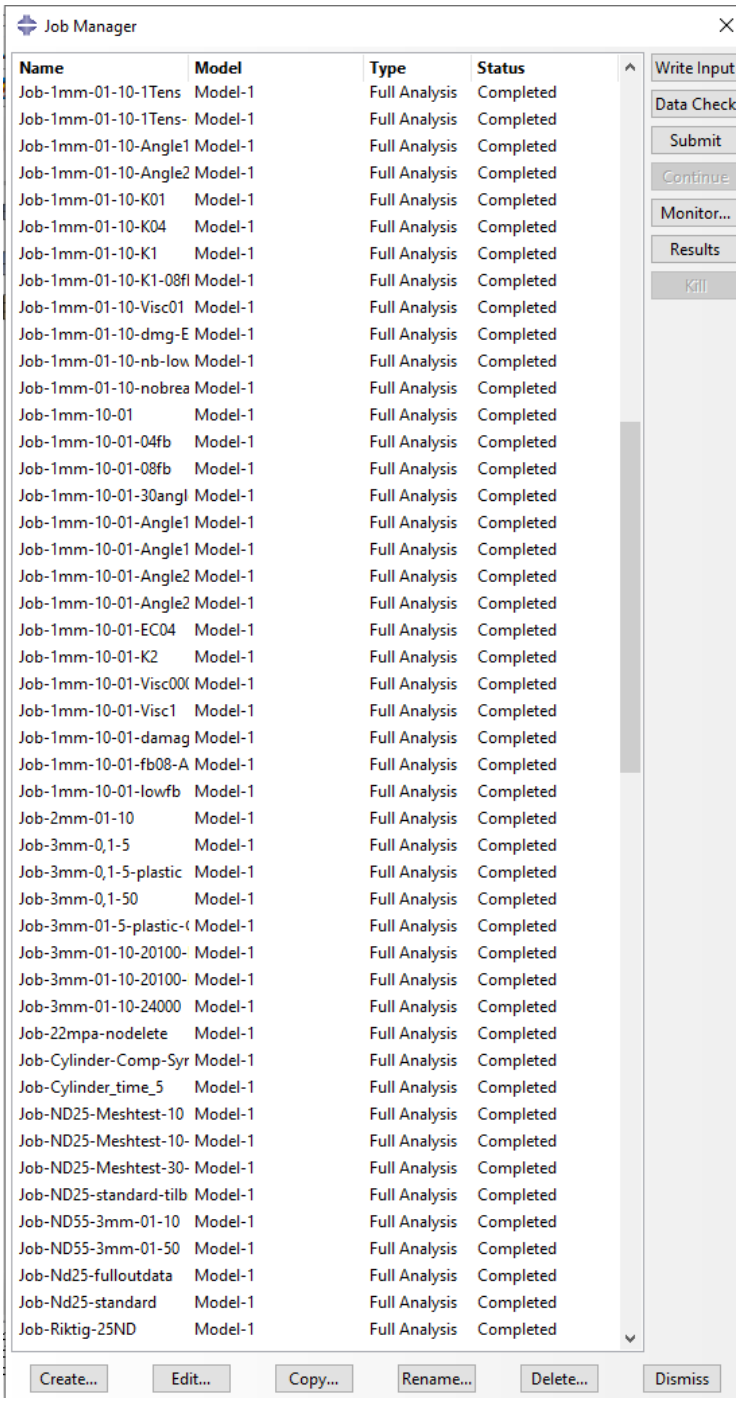
Job Manager
Name
Model
Type
Status
Job-1mm-01-10-1Tens Model-1 Full Analysis Completed
Job-1mm-01-10-1Tens- Model-1 Full Analysis Completed
Job-1mm-01-10-Angle1 Model-1 Full Analysis Completed
Job-1mm-01-10-Angle2 Model-1 Full Analysis Completed
Job-1mm-01-10-K01 Model-1 Full Analysis Completed
Job-1mm-01-10-K04 Model-1 Full Analysis Completed
Job-1mm-01-10-K1 Model-1 Full Analysis Completed
Job-1mm-01-10-K1-08fl Model-1 Full Analysis Completed
Job-1mm-01-10-Visc01 Model-1 Full Analysis Completed
Job-1mm-01-10-dmg-E Model-1 Full Analysis Completed
Job-1mm-01-10-nb-low Model-1 Full Analysis Completed
Job-1mm-01-10-nobrea Model-1 Full Analysis Completed
Job-1mm-10-01 Model-1 Full Analysis Completed
Job-1mm-10-01-04fb Model-1 Full Analysis Completed
Job-1mm-10-01-08fb Model-1 Full Analysis Completed
Job-1mm-10-01-30angl Model-1 Full Analysis Completed
Job-1mm-10-01-Angle1 Model-1 Full Analysis Completed
Job-1mm-10-01-Angle1 Model-1 Full Analysis Completed
Job-1mm-10-01-Angle2 Model-1 Full Analysis Completed
Job-1mm-10-01-Angle2 Model-1 Full Analysis Completed
Job-1mm-10-01-EC04 Model-1 Full Analysis Completed
Job-1mm-10-01-K2 Model-1 Full Analysis Completed
Job-1mm-10-01-Visc00(Model-1 Full Analysis Completed
Job-1mm-10-01-Visc1 Model-1 Full Analysis Completed
Job-1mm-10-01-damag Model-1 Full Analysis Completed
Job-1mm-10-01-fb08-A Model-1 Full Analysis Completed
Job-1mm-10-01-lowfb Model-1 Full Analysis Completed
Job-2mm-01-10 Model-1 Full Analysis Completed
Job-3mm-0,1-5 Model-1 Full Analysis Completed
Job-3mm-0,1-5-plastic Model-1 Full Analysis Completed
Job-3mm-0,1-50 Model-1 Full Analysis Completed
Job-3mm-01-5-plastic-(Model-1 Full Analysis Completed
Job-3mm-01-10-20100- Model-1 Full Analysis Completed
Job-3mm-01-10-20100- Model-1 Full Analysis Completed
Job-3mm-01-10-24000 Model-1 Full Analysis Completed
Job-22mpa-nodelete Model-1 Full Analysis Completed
Job-Cylinder-Comp-Syr Model-1 Full Analysis Completed
Job-Cylinder_time_5 Model-1 Full Analysis Completed
Job-ND25-Meshtest-10 Model-1 Full Analysis Completed
Job-ND25-Meshtest-10- Model-1 Full Analysis Completed
Job-ND25-Meshtest-30- Model-1 Full Analysis Completed
Job-ND25-standard-tilb Model-1 Full Analysis Completed
Job-ND55-3mm-01-10 Model-1 Full Analysis Completed
Job-ND55-3mm-01-50 Model-1 Full Analysis Completed
Job-Nd25-fulloutdata Model-1 Full Analysis Completed
Job-Nd25-standard Model-1 Full Analysis Completed
Job-Riktig-25ND Model-1 Full Analysis Completed
Write Input
Data Check
Submit
Continue
Monitor...
Results
Kill
Create...
Edit...
Copy...
Rename...
Delete...
Dismiss

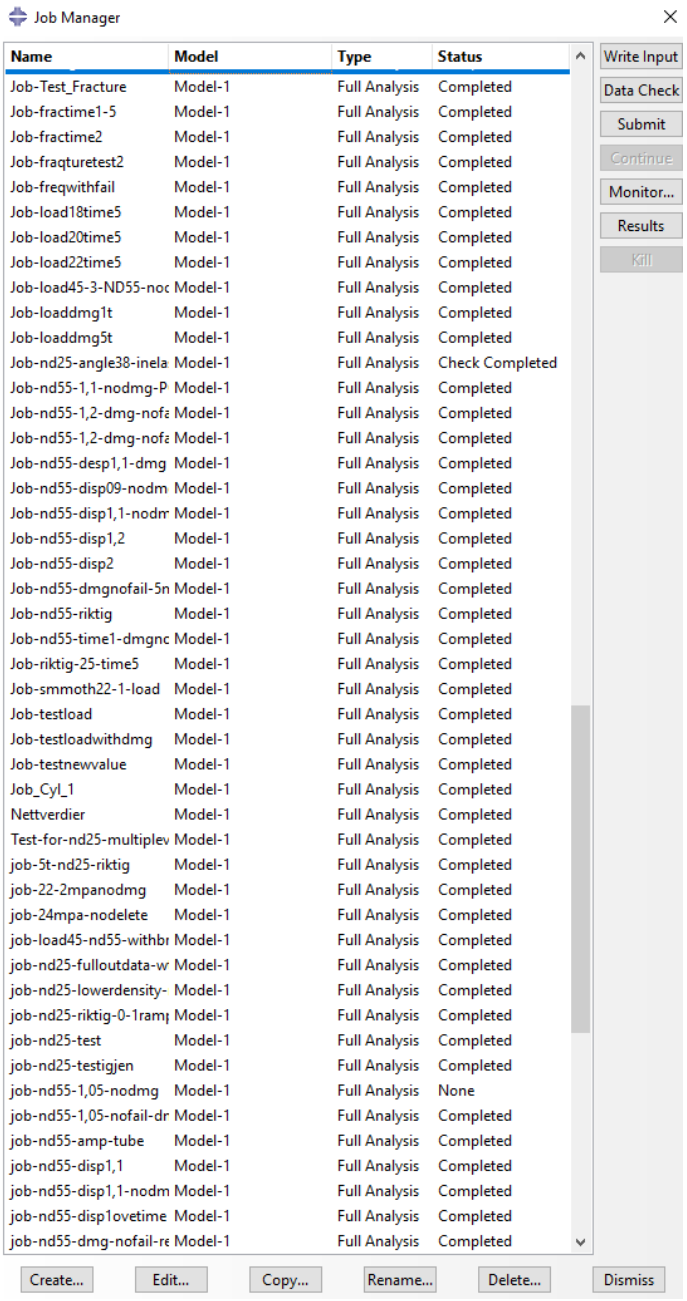
Job Manager
Name
Model
Type
Status
Job-Test_Fracture Model-1 Full Analysis Completed
Job-fractime1-5 Model-1 Full Analysis Completed
Job-fractime2 Model-1 Full Analysis Completed
Job-fraqturetest2 Model-1 Full Analysis Completed
Job-freqwithfail Model-1 Full Analysis Completed
Job-load18time5 Model-1 Full Analysis Completed
Job-load20time5 Model-1 Full Analysis Completed
Job-load22time5 Model-1 Full Analysis Completed
Job-load45-3-ND55-noc Model-1 Full Analysis Completed
Job-loaddmg1t Model-1 Full Analysis Completed
Job-loaddmg5t Model-1 Full Analysis Completed
Job-nd25-angle38-inela Model-1 Full Analysis Check Completed
Job-nd55-1,1-nodmg-P Model-1 Full Analysis Completed
Job-nd55-1,2-dmg-nofa Model-1 Full Analysis Completed
Job-nd55-1,2-dmg-nofa Model-1 Full Analysis Completed
Job-nd55-desp1,1-dmg Model-1 Full Analysis Completed
Job-nd55-disp09-nodm Model-1 Full Analysis Completed
Job-nd55-disp1,1-nodm Model-1 Full Analysis Completed
Job-nd55-disp1,2 Model-1 Full Analysis Completed
Job-nd55-disp2 Model-1 Full Analysis Completed
Job-nd55-dmgnofail-5n Model-1 Full Analysis Completed
Job-nd55-riktig Model-1 Full Analysis Completed
Job-nd55-time1-dmgnc Model-1 Full Analysis Completed
Job-riktig-25-time5 Model-1 Full Analysis Completed
Job-smmoth22-1-load Model-1 Full Analysis Completed
Job-testload Model-1 Full Analysis Completed
Job-testloadwithdmg Model-1 Full Analysis Completed
Job-testnewvalue Model-1 Full Analysis Completed
Job_Cyl_1 Model-1 Full Analysis Completed
Nettverdier Model-1 Full Analysis Completed
Test-for-nd25-multiplev Model-1 Full Analysis Completed
job-5t-nd25-riktig Model-1 Full Analysis Completed
job-22-2mpanodmg Model-1 Full Analysis Completed
job-24mpa-nodelete Model-1 Full Analysis Completed
job-load45-nd55-withb Model-1 Full Analysis Completed
job-nd25-fulloutdata-w Model-1 Full Analysis Completed
job-nd25-lowerdensity- Model-1 Full Analysis Completed
job-nd25-riktig-0-1ram Model-1 Full Analysis Completed
job-nd25-test Model-1 Full Analysis Completed
job-nd25-testigjen Model-1 Full Analysis Completed
job-nd55-1,05-nodmg Model-1 Full Analysis None
job-nd55-1,05-nofail-dr Model-1 Full Analysis Completed
job-nd55-amp-tube Model-1 Full Analysis Completed
job-nd55-disp1,1 Model-1 Full Analysis Completed
job-nd55-disp1,1-nodm Model-1 Full Analysis Completed
job-nd55-disp1ovetime Model-1 Full Analysis Completed
job-nd55-dmg-nofail-re Model-1 Full Analysis Completed
Write Input
Data Check
Submit
Continue
Monitor...
Results
Kill
Create...
Edit...
Copy...
Rename...
Delete...
Dismiss

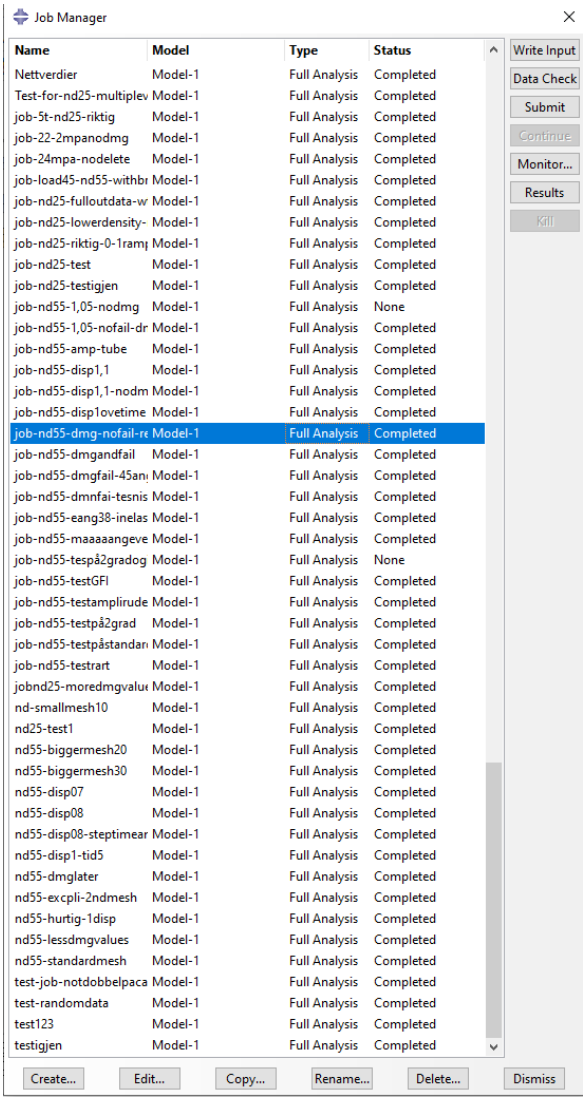
Job Manager
Name
Model
Type
Status
Nettverdier Model-1 Full Analysis Completed
Test-for-nd25-multiplev Model-1 Full Analysis Completed
job-5t-nd25-riktig Model-1 Full Analysis Completed
job-22-2mpanodmg Model-1 Full Analysis Completed
job-24mpa-nodelete Model-1 Full Analysis Completed
job-load45-nd55-withbr Model-1 Full Analysis Completed
job-nd25-fulloutdata-w Model-1 Full Analysis Completed
job-nd25-lowerdensity- Model-1 Full Analysis Completed
job-nd25-riktig-0-1ramp Model-1 Full Analysis Completed
job-nd25-test Model-1 Full Analysis Completed
job-nd25-testigjen Model-1 Full Analysis Completed
job-nd55-1,05-nodmg Model-1 Full Analysis None
job-nd55-1,05-nofail-dr Model-1 Full Analysis Completed
job-nd55-amp-tube Model-1 Full Analysis Completed
job-nd55-disp1,1 Model-1 Full Analysis Completed
job-nd55-disp1,1-nodm Model-1 Full Analysis Completed
job-nd55-disp1ovetime Model-1 Full Analysis Completed
job-nd55-dmg-nofail-re Model-1 Full Analysis Completed
job-nd55-dmgandfail Model-1 Full Analysis Completed
job-nd55-dmgfail-45an Model-1 Full Analysis Completed
job-nd55-dmnfai-tesnis Model-1 Full Analysis Completed
job-nd55-eang38-inelas Model-1 Full Analysis Completed
job-nd55-maaaaangeve Model-1 Full Analysis Completed
job-nd55-tespå2gradog Model-1 Full Analysis None
job-nd55-testGFI Model-1 Full Analysis Completed
job-nd55-testamplirude Model-1 Full Analysis Completed
job-nd55-testpå2grad Model-1 Full Analysis Completed
job-nd55-testpåstandar Model-1 Full Analysis Completed
job-nd55-testrart Model-1 Full Analysis Completed
jobnd25-moredmgvalu Model-1 Full Analysis Completed
nd-smallmesh10 Model-1 Full Analysis Completed
nd25-test1 Model-1 Full Analysis Completed
nd55-biggermesh20 Model-1 Full Analysis Completed
nd55-biggermesh30 Model-1 Full Analysis Completed
nd55-disp07 Model-1 Full Analysis Completed
nd55-disp08 Model-1 Full Analysis Completed
nd55-disp08-steptimear Model-1 Full Analysis Completed
nd55-disp1-tid5 Model-1 Full Analysis Completed
nd55-dmglater Model-1 Full Analysis Completed
nd55-excpli-2ndmesh Model-1 Full Analysis Completed
nd55-hurtig-1disp Model-1 Full Analysis Completed
nd55-lessdmgvalues Model-1 Full Analysis Completed
nd55-standardmesh Model-1 Full Analysis Completed
test-job-notdobbelpaca Model-1 Full Analysis Completed
test-randomdata Model-1 Full Analysis Completed
test123 Model-1 Full Analysis Completed
testigjen Model-1 Full Analysis Completed
Write Input
Data Check
Submit
Continue
Monitor...
Results
Kill
Create...
Edit...
Copy...
Rename...
Delete...
Dismiss

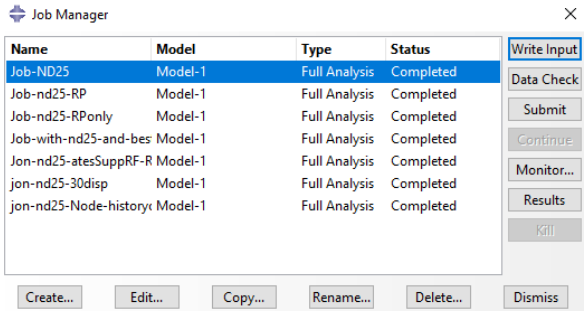
Job Manager
Name
Model
Type
Status
Job-ND25 Model-1 Full Analysis Completed
Job-nd25-RP Model-1 Full Analysis Completed
Job-nd25-RPonly Model-1 Full Analysis Completed
Job-with-nd25-and-bes Model-1 Full Analysis Completed
Jon-nd25-atesSuppRF-R Model-1 Full Analysis Completed
jon-nd25-30disp Model-1 Full Analysis Completed
jon-nd25-Node-history Model-1 Full Analysis Completed
Write Input
Data Check
Submit
Continue
Monitor...
Results
Kill
Create...
Edit...
Copy...
Rename...
Delete...
Dismiss